HHS Public Access

Author manuscript

Drug Metab Rev. Author manuscript; available in PMC 2018 December 28.

Published in final edited form as:

Drug Metab Rev. 2015 August ; 47(3): 320–334. doi:10.3109/03602532.2015.1076438.

Regulation of UGT1A1 expression and activity by miR-491-3p*

Douglas F. Dluzen,
Department of Pharmacology, Penn State University College of Medicine, Hershey, PA 17036

Dongxiao Sun,
Department of Pharmacology, Penn State University College of Medicine, Hershey, PA 17036

Anna C. Salzberg,
Department of Public Health Sciences, Penn State University College of Medicine, Hershey, PA 17036

Nate Jones,
Department of Pharmacology, Penn State University College of Medicine, Hershey, PA 17036

Ryan T. Bushey,
Department of Pharmacology, Penn State University College of Medicine, Hershey, PA 17036

Gavin P. Robertson, and
Department of Pharmacology, Penn State University College of Medicine, Hershey, PA 17036

Philip Lazarus
Department of Pharmacology, Penn State University College of Medicine, Hershey, PA 17036; Department of Pharmaceutical Sciences, Washington State University College of Pharmacy, Spokane, WA 99212

Abstract

The UDP-glucuronosyltransferase (UGT) 1A enzymes are involved in the phase II metabolism of many important endogenous and exogenous compounds. The nine UGT1A isoforms exhibit high inter-individual differences in expression but their epigenetic regulation is not well-understood. The purpose of the present study was to examine microRNA (miRNA) regulation of hepatic UGT1A enzymes and determine if that regulation impacts enzymatic activity. *In silico* analysis identified miRNA 491–3p (miR-491–3p) as a potential regulator of the UGT1A gene family via binding to the shared UGT1A 3' untranslated region common to all UGT1A enzymes. Transfection of miR-491–3p mimic into HuH-7 cells significantly repressed UGT1A1 ($P<0.001$), UGT1A3 ($P<0.05$), and UGT1A6 ($P<0.05$) mRNA levels. For UGT1A1, this repression correlated with significantly reduced metabolism of raloxifene into raloxifene-6-glucuronide (ral-6-gluc; $P<0.01$) and raloxifene-4'-glucuronide (ral-4'-gluc; $P<0.01$). In HuH-7 cells with repressed

Corresponding author: Philip Lazarus, Ph.D., Department of Pharmaceutical Sciences, Washington State University College of Pharmacy, PO Box 1495, Spokane, WA, 99210; Phone: 509-358-7947; Fax: 509-358-7967, phil.lazarus@wsu.edu.

Authorship Contributions

Participated in research design: Dluzen, Sun, Salzberg, Jones, Bushey, Robertson, and Lazarus

Conducted experiments: Dluzen and Salzberg

Contributed new reagents or analytic tools: Dluzen, Sun, Salzberg, Jones, Bushey, Robertson and Lazarus

Performed data analysis: Dluzen, Sun, Salzberg, Jones, Bushey, and Lazarus

Wrote or contributed to writing of the manuscript: Dluzen, Sun, Salzberg, Jones, Bushey, Robertson, and Lazarus

miR-491–3p expression, there was a significant increase (~80%; $P<0.01$) in UGT1A1 mRNA and a corresponding increase in glucuronidation of raloxifene into ral-6-gluc (50%, $P<0.05$) and ral-4'-gluc (22%, $P<0.01$). Knockdown of endogenous miR-491–3p in HepG2 cells did not significantly alter UGT1A1 mRNA levels, but did increase the formation of ral-6-gluc (50%, $P<0.05$) and ral-4'-gluc (34%, $P<0.001$). A significant inverse correlation between miR-491–3p expression and both UGT1A3 ($P<0.05$) and UGT1A6 ($P<0.01$) mRNA levels was observed in a panel of normal human liver specimens, with a significant ($P<0.05$) increase in UGT1A3 and UGT1A6 mRNA levels observed in miR-491–3p non-expressing versus expressing liver specimens. These results suggest that miR-491–3p is an important factor in regulating the expression of UGT1A enzymes *in vivo*.

Introduction

MicroRNA (miRNA) are dynamic epigenetic regulators of gene expression in both normal tissue development as well as tumor biology. miRNA post-transcriptionally repress protein expression primarily by binding to the 3'-untranslated region (UTR) of target mRNA and the inhibition of protein synthesis (Guo et al., 2008; Carthew and Sontheimer, 2009). Acting as a genetic switch and/or fine-tuner of protein expression, miRNA regulation can account for not only mild (e.g. two-fold) protein repression, but can also cause mRNA destabilization to dramatically reduce protein output (Baek et al., 2008; Selbach et al., 2008; Mukherji et al., 2011).

miRNA are short, ~22-nucleotide long, single-stranded RNA species that are gene-encoded and transcribed as a primary transcript (pri-miRNA) by RNA polymerase II. Pri-miRNA form a hairpin loop structure that is recognized and processed in the nucleus and then exported to the cytoplasm as a precursor miRNA(pre-miRNA) consisting of a double-stranded duplex and stem-loop. The precursor is further processed to cleave off the stem-loop structure and the RNA duplex is then recognized by the RNA-induced silencing complex (RISC) consisting of Argonaute-2 and associated proteins, which degrades the passenger strand of the RNA duplex and leaves the mature miRNA (Carthew and Sontheimer, 2009). The mature miRNA guides RISC to target mRNA 3' UTRs (less commonly the mRNA open-reading frame or 5' UTR), with target recognition primarily driven by the hybridization of the miRNA 'seed sequence' to the mRNA target. This 'seed sequence' of a target gene is defined as nucleotides 2–8 from the 5' end of the mature miRNA strand and forms perfect complementation to its mRNA target (Bartel, 2009).

The role of miRNA in tissue development is continually being investigated, but research has shown miRNA regulation to be a major contributor to tissue and cell homeostasis (Khraiwesh et al., 2010; Liu et al., 2012), signaling (Valadi et al., 2007), and oncogenesis (Hatziapostolou et al., 2011). The impact of miRNAs on drug response has not been studied as extensively. miRNA regulate expression of several human cytochrome P450 (CYP540) phase I metabolic enzymes, including the major drug and hormone metabolizing CYPs 3A4, 2E1, 1B1, and 24 (Tsuchiya et al., 2006; Komagata et al., 2009; Pan et al., 2009; Mohri et al., 2010), but there are few studies on other phase I or II enzymes.

The UDP-glucuronosyltransferase (UGT) phase II metabolic enzyme family primarily consists of two large subfamilies, the UGT1As and 2Bs. The UGT1A family, located on chromosome 2q37, codes for nine functional protein isoforms sharing alternative 1st exons spliced to common exons 2–5. The common 5th exon contains a shared 3' UTR (Fig. 1A). The UGT2B family members, located on chromosome 4q13, are expressed as individual genes encoded by six exons each with a unique 3' UTR (Mackenzie et al., 2005; Nagar and Remmel, 2006). The UGTs are generally highly expressed in liver, the primary organ of metabolism, but are also expressed extra-hepatically in tissues such as colon, prostate, lung, pancreas, kidney, and tissues of the head and neck and other aero digestive tract tissues (Nakamura et al., 2008; Bushey and Lazarus, 2012; Jones et al., 2012). Each UGT1A gene is regulated by an individual promoter, driving tissue-specific expression. UGTs 1A1, 1A3, 1A4, 1A5, 1A6 and 1A9 are the primary hepatic isoforms while UGTs 1A7, 1A8, and 1A10 are exclusively expressed extra-hepatically (Nagar and Remmel, 2006; Nakamura et al., 2008; Izukawa et al., 2009). The UGTs prime numerous endogenous compounds including bilirubin (Bosma et al., 1994) and steroid hormones (Belanger et al., 2003), as well as exogenous compounds including drugs, chemotherapeutic agents, and carcinogens (Court et al., 2001; Kemp et al., 2002; Nagar and Blanchard, 2006; Nagar and Remmel, 2006; Chen et al., 2007; Chen et al., 2008; Balliet et al., 2009; Lazarus et al., 2009; Mizuma, 2009; Chen et al., 2010; Chen et al., 2012; Rowland et al., 2013; Sun et al., 2013), for excretion from the body by catalyzing the conjugation of a sugar moiety (e.g. glucuronide) to its substrate. The exon 1-encoded amino-termini of individual UGT enzymes determines their unique substrate-specificities; however there is a high degree of substrate over-lap between UGT family members (Nagar and Remmel, 2006; Mackenzie et al., 2010).

The UGT1A family members exhibit extensive inter-individual variability of expression that contributes to variability in patient response and toxicity (Court et al., 2001). Although polymorphisms in the UGT genes and altered transcriptional regulation can contribute to altered expression and/or activity of UGT1A enzymes (Wiener et al., 2004; Hoskins et al., 2007; Chen et al., 2010; Gallagher et al., 2010), these mechanisms do not explain the observations that UGT1A mRNA and protein levels often do not correlate (Izukawa et al., 2009; Oda et al., 2012; Ohtsuki et al., 2012) and that there is a high degree of variability in UGT mRNA and protein expression within different tissues and between different individuals (Izukawa et al., 2009; Ohno and Nakajin, 2009). Such observations suggest an epigenetic mechanism of post-transcriptional regulation may be affecting UGT protein expression. We hypothesized that miRNA regulate expression of UGT1A isoforms and that this may contribute to inter-individual variability in UGT1A expression.

The present study is the first to examine miRNA interactions within the UGT1A family of enzymes. In this study, *in silico* approaches were used to screen for possible miRNA interactions with the UGT1A family of enzymes and functional studies were then performed to examine the potential role of miRNA on UGT1A gene expression. Evidence is presented demonstrating that miR-491–3p may be an important regulator of hepatic UGT1A expression and activity.

Materials and Methods

Chemicals and reagents.

The pGL3-Promoter and pRL-TK renilla plasmids were obtained from Promega (Madison, WI). All synthesized DNA oligos used for 3' UTR amplification, site-directed mutagenesis (SDM), and polymerase chain reaction (PCR) analysis were from Integrated DNA Technologies, Inc (Coralville, IA). Lipofectamine 2000 transfection reagent was from Life Technologies (Carlsbad, CA). miRVana miRNA mimic miR-491–3p (#4464066), negative control #1 mimic (#4464058), miRVana miRNA inhibitor miR-491–3p (#4464084), and negative control #1 inhibitor (#4464076) were purchased from Ambion (Austin, TX). Uridine diphosphate glucuronic acid (UDPGA), raloxifene, alamethicin, and bovine serum albumin (BSA) were obtained from Sigma-Aldrich (St. Louis, MO). Ral-6-glucuronide (ral-6-gluc), ral-4'-glucuronde (ral-4'-gluc), raloxifene-d4, ral-6-gluc-d4, ral-4'gluc-d4, and epirubicin hydrochloride were purchased from Toronto Research Chemical (Toronto, ON, Canada). Rabbit anti-UGT2B7 and anti-calnexin antibodies were from BD Biosciences (San Jose, CA) and Cell Signaling Technologies (Danvers, MA), respectively. Goat anti-rabbit secondary antibody conjugated to hydrogen peroxidase was from Thermo Scientific (Waltham, MA). All other chemicals used were purchased from Fisher Scientific (Pittsburg, PA) unless otherwise specified.

Cell lines and Culture Conditions.

Human embryonic kidney cell line 293, human hepatocellular carcinoma cell lines HepG2 and Hep3B, human liver adenocarcinoma cell line SK-HEP-1, human prostate carcinoma cell line LNCaP, human colon adenocarcinoma cell line Caco-2, human breast adenocarcinoma cell line MCF-7, and human lung carcinoma cell line A-549 were purchased from the American Type Culture Collection (ATCC, Manassas, VA). The human hepatocellular carcinoma cell line HuH-7 was a kind gift from Dr. Jianming Hu (Penn State Hershey College of Medicine, Hershey, PA). Hep3B, HEK293, A-549, and HuH-7 cells were cultured in DMEM (Gibco, Carlsbad, CA) supplemented with 10% FBS (Atlanta Biologicals, Lawrenceville, GA) and 1% penn/strep (Gibco). HepG2 and Caco-2 cells were cultured in DMEM supplemented with 10% FBS, 1% penn/strep, and 1% non-essential amino acids (Lonza, Basel, Switzerland). SK-HEP-1 and LNCaP cells were cultured in RPMI 1640 (Gibco) supplemented with 10% FBS, 1% penn/strep, and 1% NEAA. MCF-7 cells were cultured in RPMI 1640 supplemented with 10% FBS and 1% penn/strep. All cells were grown and maintained at 37°C with 5% CO_2.

Tissues and miRNA Isolation.

Normal colon and endometrium specimens (n=5 each) were obtained from the tissue bank at Penn State University College of Medicine while normal liver specimens and their matching total RNA were obtained from the H. Lee Moffitt Cancer Center Tissue Procurement Facility (n=39). All protocols involving the collection and analysis of tissue specimens from these tissue banks were approved by the Institutional Review Boards at their respective institutions and were in accordance with assurances filed with and approved by the United States Department of Health and Human Services. Normal jejunum tissue specimens were purchased from the Sun Health Research Institute (Sun City, AZ). All tissue samples were

isolated and frozen at −70°C within 2 h post-surgery. Colon, liver, jejunum, endometrium and cell line total RNA was extracted using the RNeasy Mini Kit (Qiagen, Hilden, Germany). All total RNA samples from cell lines were subject to on-column DNAse digestion during RNA purification (Qiagen). Pooled normal breast total RNA was purchased from the Biochain Institute (Hayward, CA) while normal lung, pancreas, larynx, trachea, and kidney RNA was purchased from Clontech (Mountain View, CA) or Agilent (Santa Clara, CA). Small RNA (<200 nt) containing the miRNA fraction was isolated and purified from total RNA using the mirVana miRNA Isolation Kit (Ambion). All RNA concentrations were ascertained using a Nanodrop ND-1000 spectrophotometer (Thermo Scientific) and was eluted and stored in RNase-, DNAse-free water in a −80°C freezer.

miRNA Binding Site Predictions.

The 3’ UTR of the UGT1A enzyme locus was obtained from the UCSC Genome Browser (hg18 assembly). miRNA binding site predictions were obtained using, (i) TargetScan (Lewis et al., 2005), scored with the Total Context+ score as described in Garcia et. al (Garcia et al., 2011), and (ii) miRanda, algorithm v3.0 (Betel et al., 2008) with the following parameters: Gap Open Penalty, −8.00; Gap Extend, −2.00; Score Threshold, 50.00; Energy Threshold, −20.00 kcal/mol; Scaling Parameter, 4.00.

Quantitative Real-time (qRT)-PCR.

cDNAs were synthesized from mRNA using total RNA and the SuperScript First-Strand Synthesis Kit (Invitrogen, Carlsbad, CA). miRNA cDNAs were synthesized using the Taqman MicroRNA Reverse Transcription Kit (Ambion). Taqman gene expression assays (Applied Biosystems, Carlsbad, CA) were used to amplify UGTs 1A1 (Hs02511055_s1), 1A3 (Hs04194492_g1), 1A4 (Hs016555285_s1), 1A5 (Hs01374521_s1), 1A6 (Hs01592477_m1), 1A9 (Hs02516855_gH), RPLPO (Hs99999902_m1), and 2B7 Hs02556232_s1) in HuH-7 and HepG2 cells. Taqman miRNA assays (Ambion) were used to amplify the expression of miR-491–3p (Cat. # 4427974, ID #002360) and RNU6B (Cat #4427975, ID #001093) in all cell lines and tissue samples. PCR reactions were performed in 10 μL reactions in 384-well plates using an ABI 7900HT Sequence Detection System with incubations performed at 50°C for 2 min; 95°C for 10 min; and 40 cycles of 95°C for 15 sec, 60°C for 1 min. Reactions included 2x Universal PCR Master Mix (Applied Biosystems), Taqman gene expression primers or Taqman miRNA primers, and corresponding cDNA according to the manufacturer’s protocol. Each plate was run with negative control (no DNA template) and all assays were performed in quadruplicate. Gene expression was compared to an endogenous, internal control (RPLPO for mRNA or RNU6B for miRNA) using the $2^{-\Delta\Delta C_T}$ method (Livak and Schmittgen, 2001). C_T values were determined using the SDS 2.4 software (Applied Biosystems) and amplification C_T values higher than 36 cycles were designated as below the limit of detection (B.L.D.). Samples lacking any amplification curves were also designated B.L.D.

Construction of reporter plasmids.

The luciferase report plasmids used in this study were constructed by inserting the common UGT1A 3’ UTR into the *XbaI* restriction site located downstream of the luciferase reporter gene in the pGL3-Promoter vector. Briefly, primers (sense, 5’-

GCTATCTAGAGAAGTGGGTGGGAAATAAGGTAA-3'; and antisense, 5'-GCTATCTAGAGAAACTTGCCCAGCACTTCATAGCT-3') modified with the *XbaI* digestion site at both ends were used to amplify the UGT1A subfamily 3' UTR (corresponding to nucleotides +1618 to +2301 of the human UGT1A1 mRNA, and 683 nucleotides in length) using genomic DNA isolated from the HEK293 cell line. The PCR-amplified region was cloned into the *XbaI* restriction site of the pGL3-promoter vector using standard protocols. The pGL3-seed deletion plasmid was created by performing SDM using the QuikChange II Site Directed Mutagenesis Kit (Agilent, Santa Clara, CA) and the sense and antisense primers '5-TCATTTTATTCTTATTAAG-GAAATACTTTAAATTAATCAGCCCCAGAGTGCTT-3' and 5'-AAGCACTCTGGGGCTGATTA-ATTTAAAGTATTTCCTTAATAAGAATAAAATGA-3', respectively. Nucleotide sequences of all plasmids used in this study were confirmed by DNA sequencing analysis performed at the Penn State University Nucleic Acid Facility (State College, PA).

Luciferase Assays.

The pGL3-Promoter vector cloned with the UGT1A 3' UTR (termed 'pGL3-UGT1A3'UTR') was co-transfected with the pRL-TK renilla control vector into HEK293 cells. The day before transfection, HEK293 cells were seeded onto 24-well plates at a density of approximately 50,000 cells/well, and after 24 h, 380 ng of pGL3-UGT1A3'UTR plasmid and 20 ng pRL-TK plasmid were co-transfected together with various concentrations of either scrambled miRNA control or miRNA mimic using Lipofectamine 2000 transfection reagent. HEK293 cells were harvested 24 h after transfection using passive lysis buffer, and luciferase activity was measured with a luminometor (Bio-tek Synergy HT, Winooski, VT) using the Dual-Luciferase Reporter Assay System (Promega, Madison, WI). Renilla luciferase served as the internal control.

Glucuronidation Assays.

Preparation of cell homogenates for glucuronidation activity assays was performed as previously described (Dellinger et al., 2007) after cells were transfected with 50 uL Lipofectamine 2000 in 10 cm dishes for 48 h according to manufacturerer's protocol. HuH-7 or HepG2 cells were transfected with either 50 nM scrambled miRNA controls, 50 nM miR-491–3p mimic, or 50 nM miR-491–3p inhibitor. Collected cell pellets were freeze-thawed 3x in liquid nitrogen and subjugated to 3× 10-sec pulses using a hand-held Bio-Vortexer (Biospec, Bartlesville, OK) prior to storing of 50 μL aliquots at −80°C. Protein concentrations within the cell homogenates were quantified using the BCA Protein Assay Kit (Pierce Chemical, Rockford, IL) and measured using an Appliskan Luminometor and SkanIT Software v2.3 (Thermo Scientific).

The glucuronidation assays using homogenates from HuH-7 and HepG2 cells were performed essentially as described previously (Sun et al., 2007; Sun et al., 2013). HuH-7 and HepG2 cell homogenate (100–300 μg) was incubated with 50 μM raloxifene for 90 min, or 500 μM epirubicin hydrochloride for 60 min. Raloxifene glucuronidation reactions were terminated by the addition of 25 μL cold 100% acetonitrile and centrifuged before the drying of the supernatant in a speedvac and reconstitution in 40 μL of 1:1 water:acetonitrile;

epirubicin reactions were terminated in the presence of 25 μL of cold 100% acetonitrile, centrifuged for 20 min at 13,000 g and supernatant was collected for analysis on UPLC/MS/MS.

Stock solutions of raloxifene, ral-6-Gluc, and ral-4'-Gluc and their deuterated internal standards were prepared in DMSO. Raloxifene, ral-6-Gluc, and ral-4'-Gluc were combined into a standard stock solution with final concentrations of 25 μg/mL, 100 μg/mL, and 100 μg/mL, respectively. Deuterated internal standards were combined in DMSO to final working concentrations of 50 μg/mL for raloxifene, ral-6-Gluc, and ral-4'-Gluc. The combined standard solution was then serially diluted in 1:1 water:acetonitrile to make standard working solutions from 50 ng/mL-51.2 μg/mL for raloxifene, and 1.25 ng/mL-1.28 μg/mL for ral-6-Gluc and ral-4'-Gluc. Standard calibration samples were prepared daily by spiking 1.0 μL of the combined internal standard into each of the serial-diluted working solutions (500 ng/mL final concentrations for each deuterated internal standard). All solutions were kept at −20°C before use.

Calibration standards as well as formed raloxifene and epirubicin glucuronides were analyzed using a Waters ACQUITY ultra-pressure liquid chromatography-UV detector (UPLC/UV) system (Milford, MA) with a 1.7 μ ACQUITY UPLIC BEH C18 analytical column (2.1 mm x 50 mm, Waters, Ireland) in series with a 0.2 μm Waters assay frit filter (2.1 mm). Raloxifene gradient elution conditions were performed as previously described (Sun et al., 2013). Epirubicin gradient elution conditions were performed using a flow rate of 0.5 mL/min, starting with 95% Buffer A (0.1% formic acid in water) and 5% Buffer B (0.1% formic acid in acetonitrile) for 30 sec, a subsequent linear gradient to 50% Buffer B over 2.5 min, and then 100% Buffer B maintained over the next 2 min. Raloxifene and epirubicin glucuronides were confirmed by their sensitivity to the treatment of β-glucuronidase.

Quantification of raloxifene, ral-6-gluc, and ral-4'-gluc was performed as previously described (Sun et al., 2013). Quantification of epirubicin and epirubicin-glucuronide was determined based on the ratio of epirubicin-glucuronide versus unconjugated epirubicin after calculating the area under the curve for the epirubicin-glucuronide and epirubicin peaks using a known amount of epirubicin in each reaction as a reference. Data was quantified using the MassLynxTM NT 4.1 software with QuanLynx™ program (Waters). All standard curves were constructed by plotting the ratio of analyte peak area to corresponding internal standard peak area. All experiments were performed in triplicate in independent assays.

Western blot analysis.

UGT2B7 protein levels were determined via immunoblotting. HuH-7 and HepG2 protein homogenate was adjusted to equal volumes of loading buffer and heated at 90°C for 10 min. Samples were run at 90 V on a 10% acrylamide gel and transferred to a polyvinylidene diflouride (PVDF) membrane for 2 h at 33 V. PVDF membranes were blocked in 5% milk in TBS with Tween-20 (TBS-T) for 1 h, probed with UGT2B7 or calnexin primary antibody (1:1000 dilution for each) overnight at 4°C, washed 3x in TBS-T, followed by goat anti-rabbit secondary antibody (1:5000 dilution). Protein bands were visualized using the Amersham ECL Prime Western Blotting Detection Reagent (GE Healthcare, Pittsburgh, PA)

and Hyoblot CL autoradiography film (Denville Scientific, Metuchen, NJ). Calnexin expression levels served as a loading control.

Statistical Analysis.

Statistical analysis was performed using Graphpad Prism 5 software (La Jolla, CA). For studies involving miR-491–3p miRNA mimic or miR-491–3p inhibitors, the Student's t-test (two-tailed) was used to compare experimental groups with scrambled miRNA controls. For statistical analysis of expression levels of genes labeled B.L.D., a Ct value of 40 was assigned to generate the necessary $2^{-\Delta\Delta C_T}$ values needed for statistical comparison. For the analysis of UGT1A1, 1A3, 1A6, and 1A9 vs. miR-491–3p mRNA expression in human liver specimens, a one-tailed Spearman correlation was used. In this analysis, for those specimens with no miR-491–3p expression, they were assigned a Ct value half that of the lowest miR-491–3p expressing liver specimen. For comparison of UGT1A1, 1A3, 1A6, and 1A9 mRNA levels in miR-491–3p-expressing vs. non-expressing human liver specimens, the one-tailed Mann Whitney t-test was used. *P*-values <0.05 were considered statistically significant.

Results

In silico analysis of miRNA binding to UGT1A mRNA.

The human UGT1A gene locus consists of nine alternative first exons spliced to common exons 2–5, with all nine UGT1A enzymes sharing the same 3' UTR (Fig. 1A). The mRNA corresponding to the UGT1A 3'UTR was analyzed by the miRanda (v3.0) and TargetScan algorithms to identify miRNAs that could potentially target UGT1A mRNAs (Enright et al., 2003; John et al., 2004; Lewis et al., 2005). miRanda is an excellent model algorithm due to its emphasis on stringent base-pairing of the seed region supplemented by downstream binding near the 3' end of the miRNA gene (Betel et al., 2008). TargetScan is a similarly effective model algorithm due to its emphasis on contributions from binding position, 3' pairing, and miRNA target site abundance (Garcia et al., 2011). miRNA 491–3p (miR-491–3p) was the highest scoring prediction by miRanda to bind the UGT1A common 3' UTR, followed by miR-148a and miR-136. TargetScan also identified these three miRNAs as strong candidates to bind the UGT1A 3' UTR, with miR-491–3p having the highest overall total context+ score of the three miRNAs. miR-491–3p targets the common UGT1A 3' UTR at a position 92–114 base pairs (bp) downstream of the UGT1A stop codon [termed the miR-491–3p miRNA recognition element (MRE)] (Fig. 1B). This predicted MRE contains the canonical 8-nucleotide miRNA "seed" sequence of perfect complementation between miR-491–3p and the UGT1A 3' UTR (Fig. 1B, bottom, underlined). The MREs for miRs 148a and miR-136 target regions corresponding to bp 512–533 and 610–633, respectively, downstream of the UGT1A stop codon. Like that observed for miR-491–3p, both contain a 8-nucleotide "seed" sequence of perfect complementation with the UGT1A 3' UTR (Fig. 1B, bottom, underlined).

Effect of miR-491–3p on UGT1A 3' UTR-mediated luciferase activity.

To determine whether any of the predicted miRNAs described above (miR-491–3p, miR-148a, and miR-136) could potentially affect UGT1A expression *in vitro*, the UGT1A 3'

UTR was cloned into the luciferase pGL3-promoter vector immediately 3' of the luciferase open reading frame (Fig. 1C). The pGL3-UGT1A3'UTR plasmid was transiently co-transfected into HEK293 cells with scrambled negative control or miR-491–3p, miR-148a, or miR-136 miRNA mimics together with the *renilla* luciferase plasmid (serving as a transfection control). HEK293 cells are an ideal cell line for studying heterologous expression of UGT1A enzymes since they do not exhibit endogenous UGT1A expression (Nakamura et al., 2008). Compared to the scrambled miRNA-transfected control, luciferase activity was significantly repressed at both 1 nM ($P<0.05$) and 2 nM ($P<0.05$) miR-491–3p mimic concentrations, corresponding to a 43 and 48% loss, respectively, of luciferase activity (Fig. 1D). To confirm that this inhibition was due to miRNA-491–3p binding to the UGT1A 3' UTR miR-491–3p MRE, a 4-bp deletion mutation was created within the MRE seed sequence within the pGL3-UGT1A3'UTR (termed 'pGL3-UGT1A3'UTR/SeedDel; Fig. 1C). While no significant difference in luciferase activity was observed between the seed deletion mutant and the negative scrambled miRNA control, a significant ($P<0.05$) 1.5-fold increase in luciferase expression was observed between cells over-expressing the wild-type pGL3-UGT1A3'UTR versus cells over-expressing the mutant pGL3-UGT1A3'UTR/SeedDel plasmids using 2 nM miR-491–3p mimic (Fig. 1D). No significant alteration in luciferase activity was observed in co-transfections with either the miR-148a and miR-136 mimics (data not shown).

miR-491–3p expression in UGT-expressing tissues and cell lines.

To determine the levels of miR-491–3p expression in cells with known UGT expression, total RNA was screened from a variety of normal human tissues and cell lines by quantitative real-time (qRT)-PCR (Fig. 2). miR-491–3p expression was highest in colon (25.6 ± 5.9) followed by trachea (12.0 ± 4.0) > lung (6.5 ± 0.81) > breast (3.0 ± 1.1) > liver (1.0 ± 0.11; set as reference; Fig. 2A). Of the 39 livers analyzed, 12 exhibited no expression of miR-491–3p; of the remaining samples, up to 4.0-fold differences in miRNA-491–3p expression were observed for 26 of the samples (a 7.8-fold difference was observed for the remaining sample; Fig. 2B). High miR-491–3p expression was also observed in Hep3B, HuH-7, HepG2, and SK-HEP-1 cells, exhibiting between 6.2–15.0-fold higher levels of miRNA-491–3p expression as compared to the lowest expressing individual liver specimen (Fig. 2B). Low levels of miR-491–3p expression were observed in the Caco-2, MCF-7, HEK293 and LNCaP cell lines; no expression was detected in jejunum, pancreas, kidney, larynx, and endometrium, or in the A-549 lung carcinoma cell line (data not shown).

UGT1A expression in miR-491–3p-expressing cell lines.

To identify a hepatic cell culture model that could be used to monitor the effects of miR-491–3p on hepatic UGT1A expression, UGT1A expression was quantified by qRT-PCR in both the HuH-7 and HepG2 cell lines. UGT1A1 exhibited the highest level of expression of any hepatically-expressed UGT in both cell lines, with the levels in HuH-7 cells 40-fold higher than that observed in HepG2 cells ($P<0.001$; Fig. 2C). UGT1A1 exhibited >400- and 15-fold higher levels of expression than the next-most well-expressed UGT enzyme, UGT1A6, in HuH-7 and HepG2 cells, respectively. HuH-7 and HepG2 cells also expressed the hepatic UGTs 1A3, 1A4, and 1A9. Neither cell line expressed UGT1A5 (Fig. 2C).

Effects of miR-491–3p on UGT1A expression and glucuronidation activity.

To identify which hepatic UGT1A enzyme is regulated by miR-491–3p, HuH-7 cells were transiently transfected with miR-491–3p mimic and UGT1A mRNA levels were assayed by qRT-PCR. miR-491–3p-transfected HuH-7 cells exhibited a significant ($P<0.001$) 48% decrease in UGT1A1 mRNA levels as compared to scrambled miRNA-transfected control cells (Fig. 3A). In addition, UGTs 1A3 ($P<0.05$) and 1A6 ($P<0.05$) mRNA were also decreased in the presence of miR-491–3p, with UGT transcript levels reduced by 35% and 27%, respectively. Serving as a negative control, the levels of UGT2B7 mRNA, with its own unique 3' UTR different from the common UGT1A 3' UTR and not predicted to bind miR-491–3p, did not significantly change after miR-491–3p transfection (Fig. 3A). The expression of UGTs 1A4 and 1A9 were not significantly repressed after transfection of miR-491–3p (data not shown).

Since UGT1A1 was the only UGT1A family member that was relatively well-expressed in the miRNA-491–3p-expressing HuH-7 and HepG2 cell lines and because UGT1A1 exhibited the largest variation in UGT1A expression after miR-491–3p over-expression, the role of miR-491–3p in regulating UGT1A1 expression and activity was examined specifically. Raloxifene, a chemotherapeutic agent used in the prevention of breast cancer in postmenopausal women (Jordan et al., 2001), is exclusively metabolized by the UGT1A family of enzymes, with the major raloxifene glucuronide, ral-6-gluc, formed primarily by UGT1A1 in human liver, while both UGTs 1A1 and 1A9 contribute to hepatic ral-4'-gluc formation (Kemp et al., 2002; Mizuma, 2009; Trdan Lusin et al., 2011; Sun et al., 2013). Since UGT1A1 mRNA expression levels are ~469-fold and ~15-fold higher than UGT1A9 mRNA levels in HuH-7 and HepG2 cells respectively (Fig, 2C), levels of raloxifene glucuronidation activity can serve as a specific marker for UGT1A1 activity and overall protein expression.

As a marker of UGT1A1 activity, the levels of ral-6-gluc and ral-4'-gluc formation were monitored in homogenates from HuH-7 cells transiently transfected with miR-491–3p mimic versus scrambled miRNA-transfected controls. In HuH-7 cell homogenates, both ral-6-gluc and ral-4'-gluc formation were significantly reduced by 40% ($P<0.01$) and 38%, ($P<0.01$), respectively, after transfection of miR-491–3p mimic as compared to scrambled miRNA-transfected controls (Fig. 3B). No change in UGT2B7 protein levels were observed as determined by Western blot analysis, and no difference in UGT2B7 glucuronidation activity was observed against epirubicin, a specific substrate for UGT2B7 (Innocenti et al., 2001; Zaya et al., 2006), in the presence of miR-491–3p mimic as compared to scrambled controls (Fig. 3C). Interestingly, no effect on UGT1A1 expression or activity was observed in HepG2 cells after transfection of miR-491–3p mimic as compared to scrambled miRNA-transfected controls (results not shown).

To further examine the endogenous effect of miR-491–3p on the expression and downstream activity of UGT1A1, HuH-7 cells were transiently transfected with 100 nM miR-491–3p inhibitor for 48 h. Endogenous miR-491–3p levels were significantly ($P<0.01$) reduced to below the level of detection in the presence of inhibitor as compared to scrambled miRNA inhibitor control (Fig. 4A). UGT1A1 mRNA levels were correspondingly significantly ($P<0.01$) elevated (~80%) in the presence of inhibitor as compared to scrambled control

(Fig. 4B). This increase in UGT1A1 mRNA levels corresponded with significant increases in ral-6-gluc (50%; $P<0.05$) and ral-4'-gluc (22%; $P<0.01$) formation for HuH-7 homogenates with repressed miR-491–3p levels as compared to scrambled control inhibitor-treated cell homogenates (Fig. 4C). No differences in (i) UGT2B7 mRNA levels (Fig. 4B), (ii) UGT2B7 protein levels (Fig. 4D), or (iii) glucuronidation activity against epirubicin (Fig. 4D) were observed in HuH-7 homogenates with repressed miR-491–3p levels.

A similar pattern was observed for the same miRNA inhibitor experiments performed in HepG2 cells. Endogenous miR-491–3p levels in HepG2 cells were significantly ($P<0.001$) repressed in the presence of inhibitor when compared to scrambled control (Fig. 5A). While UGT1A1 mRNA levels were not significantly altered in the presence of repressed miR-491–3p (Fig. 5B), miR-491–3p inhibition in HepG2 cells significantly increased ral-6-gluc and ral-4'-gluc formation by nearly 50% ($P<0.05$) and 34% ($P<0.001$), respectively (Fig. 5C). No difference in, (i) UGT2B7 mRNA levels (Fig. 5B), (ii) UGT2B7 protein levels (Fig. 5D), or (iii) glucuronidation activity against epirubicin (Fig. 5D) were observed in HepG2 homogenates with repressed miR-491–3p levels.

Hepatic UGT vs. miR-491–3p expression in human liver specimens.

To assess whether there was any functional effect of miR-491–3p expression on UGT1A expression, the expression of UGTs 1A1, 1A3, 1A6, and 1A9 was examined by qRT-PCR in a panel of normal human liver specimens. A significant inverse correlation was observed between UGT1A3 mRNA and miR-491–3p expression levels in 38 liver specimens which expressed UGT1A3 (Spearman $r = -0.296$; $P<0.05$; Fig. 6A). A significantly ($P<0.05$) higher level of UGT1A3 expression was observed in miR-491–3p non-expressers as compared to miR-491–3p expressers in these specimens (Fig. 6B). Similar to that observed for UGT1A3, a significant inverse correlation was also observed between UGT1A6 mRNA and miR-491–3p expression in the same liver specimens expressing UGT1A6 mRNA ($n=37$; Spearman $r = -0.487$; $P<0.01$; Fig. 6C). Also similar to that observed for UGT1A3, a significantly higher ($P<0.05$) level of UGT1A6 expression was observed in the miR-491–3p non-expressers as compared to expressers (Fig. 6D). No correlation existed between UGT1A1 or UGT1A9 mRNA levels and miR-491–3p expression was observed in the same panel of liver specimens, and no difference in UGT1A1 or UGT1A9 mRNA levels was observed between miR-491–3p-expressing versus miR-491–3p-non-expressing liver specimens (results not shown).

Discussion

This is the first study to examine the regulation of the UGT family of enzymes by miRNA. *In silico* prediction modeling using both miRanda and TargetScan indicated that miR-491–3p was the top candidate to bind to the UGT1A 3' UTR. While miR-491–3p and two other top candidate miRNAs (miR-148a and miR-136) were tested using the luciferase reporter assay, only miR-491–3p repressed luciferase activity *in vitro*. These data were further confirmed in the UGT1A1-expressing HuH-7 cell line, as miR-491–3p over-expression was shown to significantly inhibit UGT1A1 expression and glucuronidation activity, while inhibition of miR-491–3p was shown to significantly induce UGT1A1 expression and

glucuronidation activity. In addition, deletion of the seed sequence within the 3' UTR miR-491–3p MRE of the UGT1A1 gene resulted in an elimination of these effects, suggesting specificity of action.

The expression of UGTs 1A3 and 1A6 were significantly and inversely correlated with miR-491–3p expression levels in a panel of normal human liver specimens examined in this study. Furthermore, a significant difference in UGT1A3 and UGT1A6 mRNA expression was observed in liver specimens stratified by miR-491–3p-expression versus miR-491–3p-non-expression. Together, these data strongly suggest that miR-491–3p plays a role in the regulation of UGT1A expression and activity and may contribute to the observed inter-individual variability of several UGT1A genes in humans.

While a significant increase in UGT1A1 expression and enzyme activity was observed in HepG2 cells after inhibition of miRNA-491–3p, no effect on UGT1A1 mRNA levels or activity was observed in HepG2 cells after miR-491–3p over-expression. This contrasts with the inhibitory effect observed for both UGT1A1 mRNA expression and enzyme activity after miR-491–3p over-expression in HuH-7 cells. This difference is likely due to the higher miR-491–3p:UGT1A1 expression ratio observed between HepG2 and HuH-7 cells. This ratio difference is due mainly to the difference in expression of UGT1A1 in the two cell lines – UGT1A1 is expressed in HepG2 cells at levels well below (~40-fold less) that observed in HuH-7 cells; there is a ~5-fold difference in miR-491–3p expression levels between the two cell lines. In HepG2 cells where the miR-491–3p:UGT1A1 expression ratio is high, it is likely that further expression of miR-491–3p has little effect on UGT1A1 expression and subsequent activity – it may already be at saturating levels, a situation that is less likely to be observed for HuH-7 cells where the miR-491–3p:UGT1A1 expression ratio is significantly lower. When miR-491–3p is inhibited, a significant effect on UGT1A1 expression and subsequent activity would be expected in both cell lines.

While significant inverse correlations were observed between both UGT1A3 and UGT1A6 mRNA levels and miR-491–3p expression in normal human liver specimens, no such association was observed for UGT1A1. Similarly, while a significant difference in UGT1A3 and UGT1A6 mRNA expression was observed in miR-491–3p expressing versus miR-491–3p non-expressing liver specimens in this study, no difference was observed for UGT1A1 expression. The fact that no association was observed between UGT1A9 mRNA levels and miR-491–3p expression is consistent with the fact that UGT1A9 was not shown to be affected by miR-491–3p *in vitro*. Previous studies have shown that UGTs 1A3 and 1A6 are expressed at levels up to 10- and 3-fold lower, respectively, than UGT1A1 in normal human liver (Izukawa et al., 2009; Ohno and Nakajin, 2009). Similar to that described above for cell lines, the miR-491–3p:UGT1A expression ratio is therefore higher for UGT1A1 than for UGT1A3 and UGT1A6 in human liver, and changes in hepatic miR-491–3p expression may only significantly affect the lower mRNA expression of hepatic UGTs like UGTs 1A3 and 1A6. These results do not rule out the possibility that miR-491–3p regulates UGT1A1 protein expression in human liver. Future studies are required to examine the impact of miR-491–3p expression on the enzymatic activity of UGT1A1 in liver specimens over-expressing miR-491–3p.

The levels of both UGT1A1 mRNA and enzyme activity were significantly altered in HuH-7 cells whereas in HepG2 cells only UGT1A1 enzyme activity was affected after over-expression of miR-491–3p. This may reflect different cell-specific mechanisms of miR-491–3p regulation of UGT1A1 protein expression. It is likely that the alterations in UGT1A1 activity observed in HuH-7 cells are via a reduction in mRNA levels, presumably through mRNA degradation. In HepG2 cells, with no observable reduction in UGT1A1 mRNA levels after miR-491–3p over-expression, the primary mechanism of protein repression could be through translational inhibition or relocation and sequestering of UGT1A1 mRNA into P-bodies, where mRNA can be stored with RISC for later usage or until degraded (Macfarlane and Murphy, 2010). Cell-specific miRNA regulation of protein expression is observed for other genes. For example, hepatocyte nuclear factor 4 alpha (HNF4α) is regulated in HepG2 cells by miR-24 and miR-34a. Mechanistically, miR-24 reduces HNF4α protein expression primarily via mRNA degradation; whereas miR-34a primarily regulates HNF4α expression via translational inhibition (Takagi et al., 2010). In HuH-7 cells, peroxisome proliferator-activated receptor alpha (PPARα) is primarily regulated by miR-21 and miR-27b via translation inhibition (Kida et al., 2011), while in HepG2 cells PPARα is regulated by miR-141 via reduced mRNA expression levels (Hu et al., 2012). In both cases, however, the differential effect observed between cell lines was manifested by two different miRNA species. For UGT1A1, this differential cell line effect was linked to the same miRNA (miR-491–3p).

It is possible that the UGT1A 3’ UTR is not the sole region where miRNA may play a role in UGT1A regulation, as there are other genes which are regulated by miRNA predicted to bind within the 5’ untranslated or coding regions. For example, miR-24 regulates HNF4α protein expression primarily by binding within the mRNA coding region (Takagi et al., 2010). In the present studies, no effect on UGT1A glucuronidation activity was observed when levels of miR-125a-3p were altered in either HepG2 or Huh7 cells (results not shown). As miR-125a-3p was the miRNA predicted by miRanda to bind within non-3’UTR UGT1A sequences with the most efficacy, this suggests that miRNA regulation of UGT1A expression is primarily via binding to the UGT1A 3’UTR. It is also possible that the prediction programs used in this analysis (miRanda and TargetScan) failed to adequately predict the binding of other miRNA within these UGT1A sequences. miRNA-pull-down techniques using the UGT1A 3’ UTR as a probe could be used to better assess this possibility (Roff et al., 2012).

Interestingly, the expression of the hepatic UGT1A4 and UGT1A9 were not significantly regulated by miR-491–3p over-expression in the present studies. This may be due to UGT1A mRNA secondary structure potentially interfering with miR-491–3p and/or protein binding. We analyzed the mRNA secondary structures for UGTs 1A1, 1A3, 1A4, 1A6, and 1A9 using the RNA Fold software (Gruber et al., 2008) to better asses this possibility (Supplementary Fig. 1). While UGTs 1A3 and 1A4 had the most similar structure, each UGT1A isoform exhibited a unique secondary structure and this may impact miR-491–3p binding to each isoform (Supplementary Fig. 1). mRNA secondary structure can play an important role in miRNA regulation and targeting, as previous reports have identified polymorphisms within mRNA 3’ UTRs that alter miRNA regulation due to changes in

mRNA secondary structure (Haas et al., 2012). Further studies will be necessary to better assess this possibility.

While miR-491–3p was shown to be expressed hepatically, it was also shown to be expressed in several other normal human tissues including colon, lung, trachea, and breast. In fact, the expression of miR-491–3p was higher in these tissues than was observed in liver. Therefore, in addition to playing a potential role in whole-body metabolism via hepatic mechanisms, miR-491–3p could be playing an important role in regulating local metabolism within these extra-hepatic tissues. Further studies are required examining the effects of miR-491–3p on UGT1A expression for non-hepatic human tissues.

In summary, this is the first evidence demonstrating that miRNA regulate phase II UGT metabolic enzymes. Results from both *in vitro* studies in cell lines and human tissue phenotype data are presented demonstrating that UGTs including 1A3, 1A6, and possibly other UGT1A enzymes including UGT1A1 are regulated by miR-491–3p. Alterations in the expression of UGT1A enzymes by miR-491–3p may be an important mechanism controlling phase II metabolism and may play an important role in modulating drug response in humans.

Supplementary Material

Refer to Web version on PubMed Central for supplementary material.

Acknowledgements

We would like to thank the Pennsylvania State University Nucleic Acids Research Core Facility for their support and help with sequencing and PCR expression analysis. We acknowledge the assistance and help of the Penn State Hershey Cancer Institute Biorepository.

*__Funding:__ This work was funded in part by a student fellowship provided by AstraZeneca (to D Dluzen), and grants from the National Institutes of Health, National Institute of Dental and Craniofacial Research [grant R01-DE13158 to P Lazarus], the Pennsylvania Department of Health's Health Research Formula Funding Program [grant 4100038714, to P Lazarus] and the National Center for Research Resources and the National Center for Advancing Translational Sciences, National Institutes of Health, Grant UL1-TR000127.

Abbreviations:

(MS)	mass spectrometry
(miRNA)	microRNA
(qRT-PCR)	quantitative reverse-transcription polymerase chain reaction
(UGT)	UDP-glucuronosyltransferase
(UPLC)	ultra-pressure liquid chromatography
(UDPGA)	Uridine diphosphate glucuronic acid

References

Baek D, Villen J, Shin C, Camargo FD, Gygi SP and Bartel DP (2008) The impact of microRNAs on protein output. Nature 455:64–71. [PubMed: 18668037]

Balliet RM, Chen G, Gallagher CJ, Dellinger RW, Sun D and Lazarus P (2009) Characterization of UGTs active against SAHA and association between SAHA glucuronidation activity phenotype with UGT genotype. Cancer Res 69:2981–2989. [PubMed: 19318555]

Bartel DP (2009) MicroRNAs: target recognition and regulatory functions. Cell 136:215–233. [PubMed: 19167326]

Belanger A, Pelletier G, Labrie F, Barbier O and Chouinard S (2003) Inactivation of androgens by UDP-glucuronosyltransferase enzymes in humans. Trends Endocrinol Metab 14:473–479. [PubMed: 14643063]

Betel D, Wilson M, Gabow A, Marks DS and Sander C (2008) The microRNA.org resource: targets and expression. Nucleic Acids Res 36:D149–153. [PubMed: 18158296]

Bosma PJ, Seppen J, Goldhoorn B, Bakker C, Oude Elferink RP, Chowdhury JR, Chowdhury NR and Jansen PL (1994) Bilirubin UDP-glucuronosyltransferase 1 is the only relevant bilirubin glucuronidating isoform in man. J Biol Chem 269:17960–17964. [PubMed: 8027054]

Bushey RT and Lazarus P (2012) Identification and functional characterization of a novel UDP-glucuronosyltransferase 2A1 splice variant: potential importance in tobacco-related cancer susceptibility. J Pharmacol Exp Ther 343:712–724. [PubMed: 22984225]

Carthew RW and Sontheimer EJ (2009) Origins and Mechanisms of miRNAs and siRNAs. Cell 136:642–655. [PubMed: 19239886]

Chen G, Blevins-Primeau AS, Dellinger RW, Muscat JE and Lazarus P (2007) Glucuronidation of nicotine and cotinine by UGT2B10: loss of function by the UGT2B10 Codon 67 (Asp>Tyr) polymorphism. Cancer Res 67:9024–9029. [PubMed: 17909004]

Chen G, Dellinger RW, Sun D, Spratt TE and Lazarus P (2008) Glucuronidation of tobacco-specific nitrosamines by UGT2B10. Drug Metab Dispos 36:824–830. [PubMed: 18238858]

Chen G, Giambrone NE, Jr., Dluzen DF, Muscat JE, Berg A, Gallagher CJand Lazarus P (2010) Glucuronidation genotypes and nicotine metabolic phenotypes: importance of functional UGT2B10 and UGT2B17 polymorphisms. Cancer Res 70:7543–7552. [PubMed: 20876810]

Chen G, Giambrone NE and Lazarus P (2012) Glucuronidation of trans-3'-hydroxycotinine by UGT2B17 and UGT2B10. Pharmacogenet Genomics 22:183–190. [PubMed: 22228205]

Court MH, Duan SX, von Moltke LL, Greenblatt DJ, Patten CJ, Miners JO and Mackenzie PI (2001) Interindividual variability in acetaminophen glucuronidation by human liver microsomes: identification of relevant acetaminophen UDP-glucuronosyltransferase isoforms. J Pharmacol Exp Ther 299:998–1006. [PubMed: 11714888]

Dellinger RW, Chen G, Blevins-Primeau AS, Krzeminski J, Amin S and Lazarus P (2007) Glucuronidation of PhIP and N-OH-PhIP by UDP-glucuronosyltransferase 1A10. Carcinogenesis 28:2412–2418. [PubMed: 17638922]

Enright AJ, John B, Gaul U, Tuschl T, Sander C and Marks DS (2003) MicroRNA targets in Drosophila. Genome Biol 5:R1. [PubMed: 14709173]

Gallagher CJ, Balliet RM, Sun D, Chen G and Lazarus P (2010) Sex differences in UDP-glucuronosyltransferase 2B17 expression and activity. Drug Metab Dispos 38:2204–2209. [PubMed: 20810538]

Garcia DM, Baek D, Shin C, Bell GW, Grimson A and Bartel DP (2011) Weak seed-pairing stability and high target-site abundance decrease the proficiency of lsy-6 and other microRNAs. Nat Struct Mol Biol 18:1139–1146. [PubMed: 21909094]

Gruber AR, Lorenz R, Bernhart SH, Neubock R and Hofacker IL (2008) The Vienna RNA websuite. Nucleic Acids Res 36:W70–74. [PubMed: 18424795]

Guo H, Ingolia NT, Weissman JS and Bartel DP (2008) Mammalian microRNAs predominantly act to decrease target mRNA levels. Nature 466:835–840.

Haas U, Sczakiel G and Laufer SD (2012) MicroRNA-mediated regulation of gene expression is affected by disease-associated SNPs within the 3'-UTR via altered RNA structure. RNA biology 9:924–937. [PubMed: 22664914]

Hatziapostolou M, Polytarchou C, Aggelidou E, Drakaki A, Poultsides GA, Jaeger SA, Ogata H, Karin M, Struhl K, Hadzopoulou-Cladaras M and Iliopoulos D (2011) An HNF4alpha-miRNA inflammatory feedback circuit regulates hepatocellular oncogenesis. Cell 147:1233–1247. [PubMed: 22153071]

Hoskins JM, Goldberg RM, Qu P, Ibrahim JG and McLeod HL (2007) UGT1A1*28 genotype and irinotecan-induced neutropenia: dose matters. J Natl Cancer Inst 99:1290–1295. [PubMed: 17728214]

Hu W, Wang X, Ding X, Li Y, Zhang X, Xie P, Yang J and Wang S (2012) MicroRNA-141 represses HBV replication by targeting PPARA. PLoS One 7:e34165. [PubMed: 22479552]

Innocenti F, Iyer L, Ramirez J, Green MD and Ratain MJ (2001) Epirubicin glucuronidation is catalyzed by human UDP-glucuronosyltransferase 2B7. Drug Metab Dispos 29:686–692. [PubMed: 11302935]

Izukawa T, Nakajima M, Fujiwara R, Yamanaka H, Fukami T, Takamiya M, Aoki Y, Ikushiro S, Sakaki T and Yokoi T (2009) Quantitative analysis of UDP-glucuronosyltransferase (UGT) 1A and UGT2B expression levels in human livers. Drug Metab Dispos 37:1759–1768. [PubMed: 19439486]

John B, Enright AJ, Aravin A, Tuschl T, Sander C and Marks DS (2004) Human MicroRNA targets. PLoS Biol 2:e363. [PubMed: 15502875]

Jones NR, Sun D, Freeman WM and Lazarus P (2012) Quantification of Hepatic UDP glucuronosyltransferase 1A splice variant expression and correlation of UDP glucuronosyltransferase 1A1 variant expression with glucuronidation activity. J Pharmacol Exp Ther 342:720–729. [PubMed: 22661630]

Jordan VC, Gapstur S and Morrow M (2001) Selective estrogen receptor modulation and reduction in risk of breast cancer, osteoporosis, and coronary heart disease. J Natl Cancer Inst 93:1449–1457. [PubMed: 11584060]

Kemp DC, Fan PW and Stevens JC (2002) Characterization of raloxifene glucuronidation in vitro: contribution of intestinal metabolism to presystemic clearance. Drug Metab Dispos 30:694–700. [PubMed: 12019197]

Khraiwesh B, Arif MA, Seumel GI, Ossowski S, Weigel D, Reski R and Frank W (2010) Transcriptional control of gene expression by microRNAs. Cell 140:111–122. [PubMed: 20085706]

Kida K, Nakajima M, Mohri T, Oda Y, Takagi S, Fukami T and Yokoi T (2011) PPARalpha is regulated by miR-21 and miR-27b in human liver. Pharm Res 28:2467–2476. [PubMed: 21562928]

Komagata S, Nakajima M, Takagi S, Mohri T, Taniya T and Yokoi T (2009) Human CYP24 catalyzing the inactivation of calcitriol is post-transcriptionally regulated by miR-125b. Mol Pharmacol 76:702–709. [PubMed: 19570947]

Lazarus P, Blevins-Primeau AS, Zheng Y and Sun D (2009) Potential role of UGT pharmacogenetics in cancer treatment and prevention: focus on tamoxifen. Ann N Y Acad Sci 1155:99–111. [PubMed: 19250197]

Lewis BP, Burge CB and Bartel DP (2005) Conserved seed pairing, often flanked by adenosines, indicates that thousands of human genes are microRNA targets. Cell 120:15–20. [PubMed: 15652477]

Liu DZ, Ander BP, Tian Y, Stamova B, Jickling GC, Davis RR and Sharp FR (2012) Integrated analysis of mRNA and microRNA expression in mature neurons, neural progenitor cells and neuroblastoma cells. Gene 495:120–127. [PubMed: 22244746]

Livak KJ and Schmittgen TD (2001) Analysis of relative gene expression data using real-time quantitative PCR and the 2(-Delta Delta C(T)) Method. Methods 25:402–408. [PubMed: 11846609]

Macfarlane LA and Murphy PR (2010) MicroRNA: Biogenesis, Function and Role in Cancer. Curr Genomics 11:537–561. [PubMed: 21532838]

Mackenzie PI, Bock KW, Burchell B, Guillemette C, Ikushiro S, Iyanagi T, Miners JO, Owens IS and Nebert DW (2005) Nomenclature update for the mammalian UDP glycosyltransferase (UGT) gene superfamily. Pharmacogenet Genomics 15:677–685. [PubMed: 16141793]

Mackenzie PI, Hu DG and Gardner-Stephen DA (2010) The regulation of UDP-glucuronosyltransferase genes by tissue-specific and ligand-activated transcription factors. Drug Metab Rev 42:99–109. [PubMed: 20070244]

Mizuma T (2009) Intestinal glucuronidation metabolism may have a greater impact on oral bioavailability than hepatic glucuronidation metabolism in humans: a study with raloxifene, substrate for UGT1A1, 1A8, 1A9, and 1A10. International journal of pharmaceutics 378:140–141. [PubMed: 19486934]

Mohri T, Nakajima M, Fukami T, Takamiya M, Aoki Y and Yokoi T (2010) Human CYP2E1 is regulated by miR-378. Biochem Pharmacol 79:1045–1052. [PubMed: 19945440]

Mukherji S, Ebert MS, Zheng GX, Tsang JS, Sharp PA and van Oudenaarden A (2011) MicroRNAs can generate thresholds in target gene expression. Nat Genet 43:854–859. [PubMed: 21857679]

Nagar S and Blanchard RL (2006) Pharmacogenetics of uridine diphosphoglucuronosyltransferase (UGT) 1A family members and its role in patient response to irinotecan. Drug Metab Rev 38:393–409. [PubMed: 16877259]

Nagar S and Remmel RP (2006) Uridine diphosphoglucuronosyltransferase pharmacogenetics and cancer. Oncogene 25:1659–1672. [PubMed: 16550166]

Nakamura A, Nakajima M, Yamanaka H, Fujiwara R and Yokoi T (2008) Expression of UGT1A and UGT2B mRNA in human normal tissues and various cell lines. Drug Metab Dispos 36:1461–1464. [PubMed: 18480185]

Oda S, Nakajima M, Hatakeyama M, Fukami T and Yokoi T (2012) Preparation of a specific monoclonal antibody against human UDP-glucuronosyltransferase (UGT) 1A9 and evaluation of UGT1A9 protein levels in human tissues. Drug Metab Dispos 40:1620–1627. [PubMed: 22619308]

Ohno S and Nakajin S (2009) Determination of mRNA expression of human UDP-glucuronosyltransferases and application for localization in various human tissues by real-time reverse transcriptase-polymerase chain reaction. Drug Metab Dispos 37:32–40. [PubMed: 18838504]

Ohtsuki S, Schaefer O, Kawakami H, Inoue T, Liehner S, Saito A, Ishiguro N, Kishimoto W, Ludwig-Schwellinger E, Ebner T and Terasaki T (2012) Simultaneous absolute protein quantification of transporters, cytochromes P450, and UDP-glucuronosyltransferases as a novel approach for the characterization of individual human liver: comparison with mRNA levels and activities. Drug Metab Dispos 40:83–92. [PubMed: 21994437]

Pan YZ, Gao W and Yu AM (2009) MicroRNAs regulate CYP3A4 expression via direct and indirect targeting. Drug Metab Dispos 37:2112–2117. [PubMed: 19581388]

Roff AN, Panganiban RP, Bond JS and Ishmael FT (2012) Post-transcriptional regulation of meprin alpha by the RNA-binding proteins Hu antigen R (HuR) and tristetraprolin (TTP). J Biol Chem 288:4733–4743. [PubMed: 23269677]

Rowland A, Miners JO and Mackenzie PI (2013) The UDP-glucuronosyltransferases: Their role in drug metabolism and detoxification. Int J Biochem Cell Biol 45:1121–1132. [PubMed: 23500526]

Selbach M, Schwanhausser B, Thierfelder N, Fang Z, Khanin R and Rajewsky N (2008) Widespread changes in protein synthesis induced by microRNAs. Nature 455:58–63. [PubMed: 18668040]

Sun D, Jones NR, Manni A and Lazarus P (2013) Characterization of raloxifene glucuronidation. Potential role of UGT1A8 genotype on raloxifene metabolism in vivo. Cancer Prev Res (Phila).

Sun D, Sharma AK, Dellinger RW, Blevins-Primeau AS, Balliet RM, Chen G, Boyiri T, Amin S and Lazarus P (2007) Glucuronidation of active tamoxifen metabolites by the human UDP glucuronosyltransferases. Drug Metab Dispos 35:2006–2014. [PubMed: 17664247]

Takagi S, Nakajima M, Kida K, Yamaura Y, Fukami T and Yokoi T (2010) MicroRNAs regulate human hepatocyte nuclear factor 4alpha, modulating the expression of metabolic enzymes and cell cycle. J Biol Chem 285:4415–4422. [PubMed: 20018894]

Trdan Lusin T, Trontelj J and Mrhar A (2011) Raloxifene glucuronidation in human intestine, kidney, and liver microsomes and in human liver microsomes genotyped for the UGT1A1*28 polymorphism. Drug Metab Dispos 39:2347–2354. [PubMed: 21937736]

Tsuchiya Y, Nakajima M, Takagi S, Taniya T and Yokoi T (2006) MicroRNA regulates the expression of human cytochrome P450 1B1. Cancer Res 66:9090–9098. [PubMed: 16982751]

Valadi H, Ekstrom K, Bossios A, Sjostrand M, Lee JJ and Lotvall JO (2007) Exosome-mediated transfer of mRNAs and microRNAs is a novel mechanism of genetic exchange between cells. Nat Cell Biol 9:654–659. [PubMed: 17486113]

Wiener D, Fang JL, Dossett N and Lazarus P (2004) Correlation between UDP-glucuronosyltransferase genotypes and 4-(methylnitrosamino)-1-(3-pyridyl)-1-butanone glucuronidation phenotype in human liver microsomes. Cancer Res 64:1190–1196. [PubMed: 14871856]

Zaya MJ, Hines RN and Stevens JC (2006) Epirubicin glucuronidation and UGT2B7 developmental expression. Drug Metab Dispos 34:2097–2101. [PubMed: 16985101]

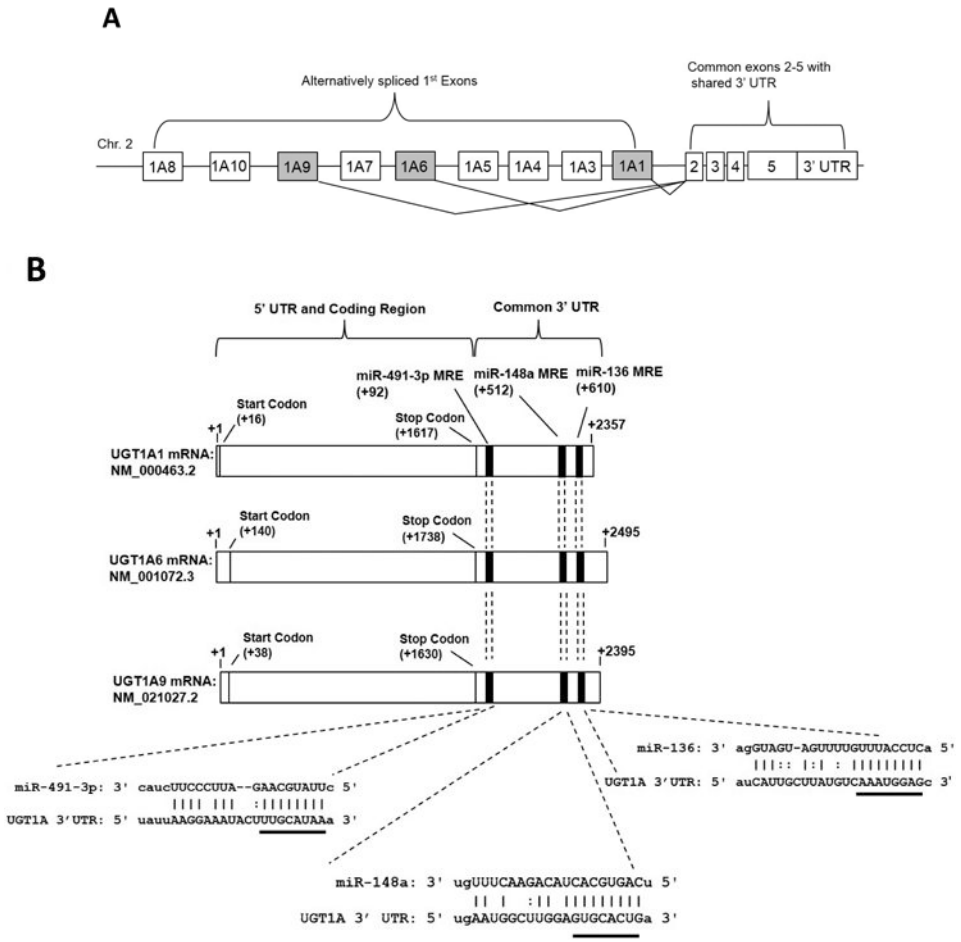

C

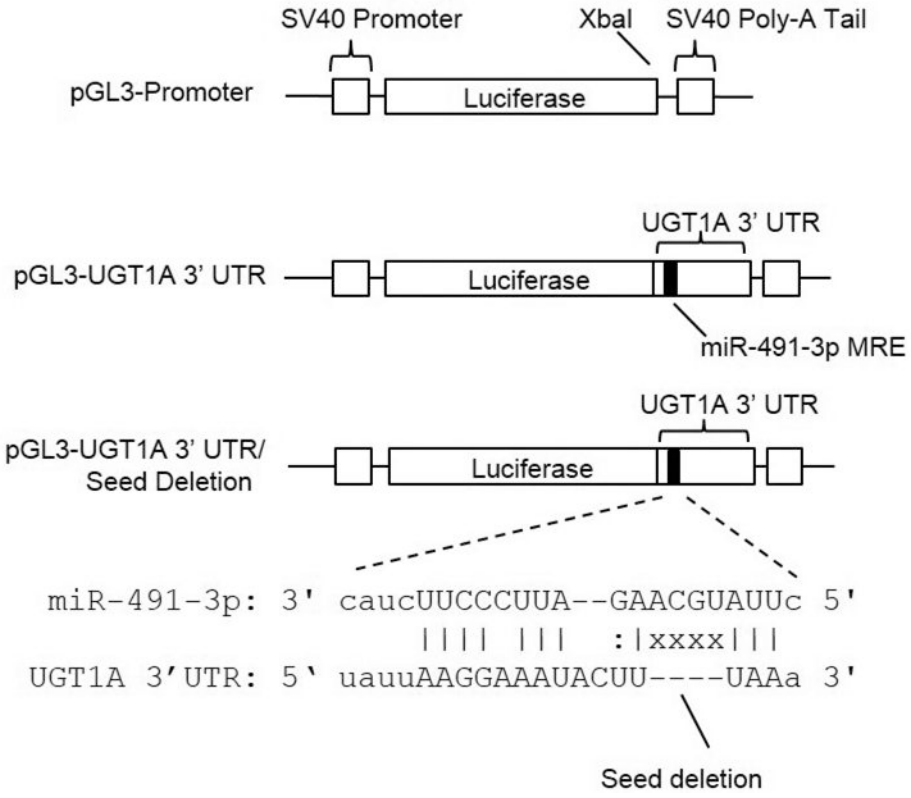

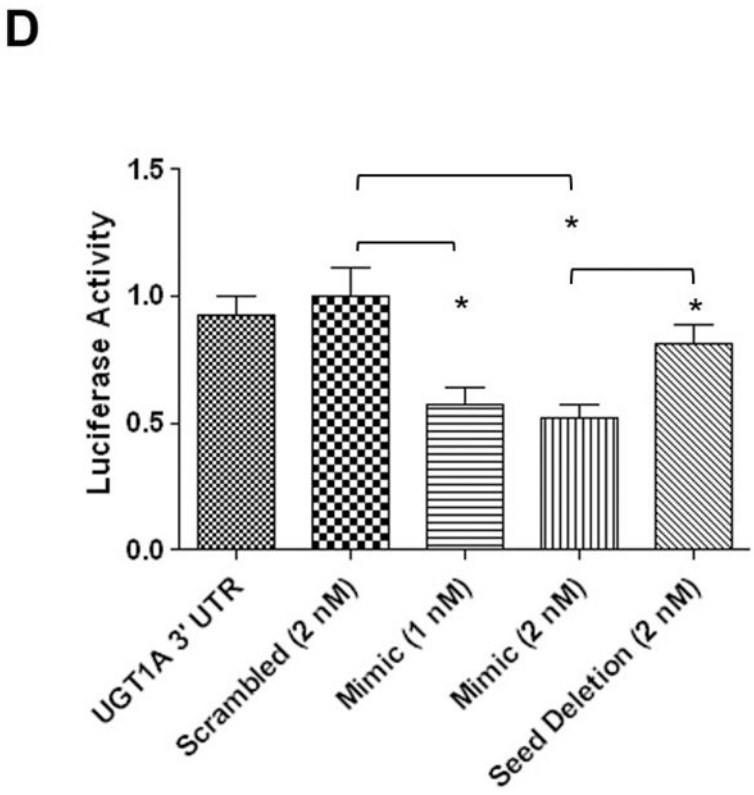

Figure 1. The UGT1A gene locus and potential miR-491–3p miRNA recognition elements (MRE) within the common UGT1A 3' UTR.

A, The 9 alternative UGT1A first exons code for unique enzymes. UGTs 1A1, 1A6, and 1A9 (dark boxes) are further highlighted in panel B. *B,* Alignment of three representative UGT1A mRNAs (1A1, 1A6, and 1A9) to highlight the common 3' UTR region. The miR-491–3p MRE begins +92 nucleotides from the stop codon for all UGT enzymes and the region spans 24 nucleotides in length. The miR-148a (spanning 22 nucleotides) and miR-136 (spanning 24 nucleotides) MREs begin at +512 and +610 nucleotides, respectively, from the stop codon. The predicted hybridization structure between the UGT1A 3' UTR and the miR-491–3p, miR-148a, and miR-136 MREs are enlarged at the bottom. Highlighted above the black bars are the MRE 'seed' sequences. *C,* Schematic of the pGL3-Promoter luciferase vector with the SV40 promoter and the SV40 poly-A tail, including the *XbaI* 3' UTR restriction digest cloning site. The pGL3-UGT1A 3'UTR luciferase vector contains the first 683 nucleotides of the UGT1A family 3' UTR, encompassing the wild-type miR-491–3p MRE. The pGL3-UGT1A 3'UTR/Seed Deletion vector contains all sequences of the pGL3-UGT1A 3' UTR vector except for a four nucleotide deletion within the miR-491–3p MRE 'seed sequence'. X's indicate deleted base positions. *D,* Luciferase activity of UGT1A 3' UTR luciferase reporter vectors co-transfected with miR-491–3p mimic or scrambled miRNA control in HEK293 cells. Columns represent mean ± S.E. of three independent experiments. * $P<0.05$.

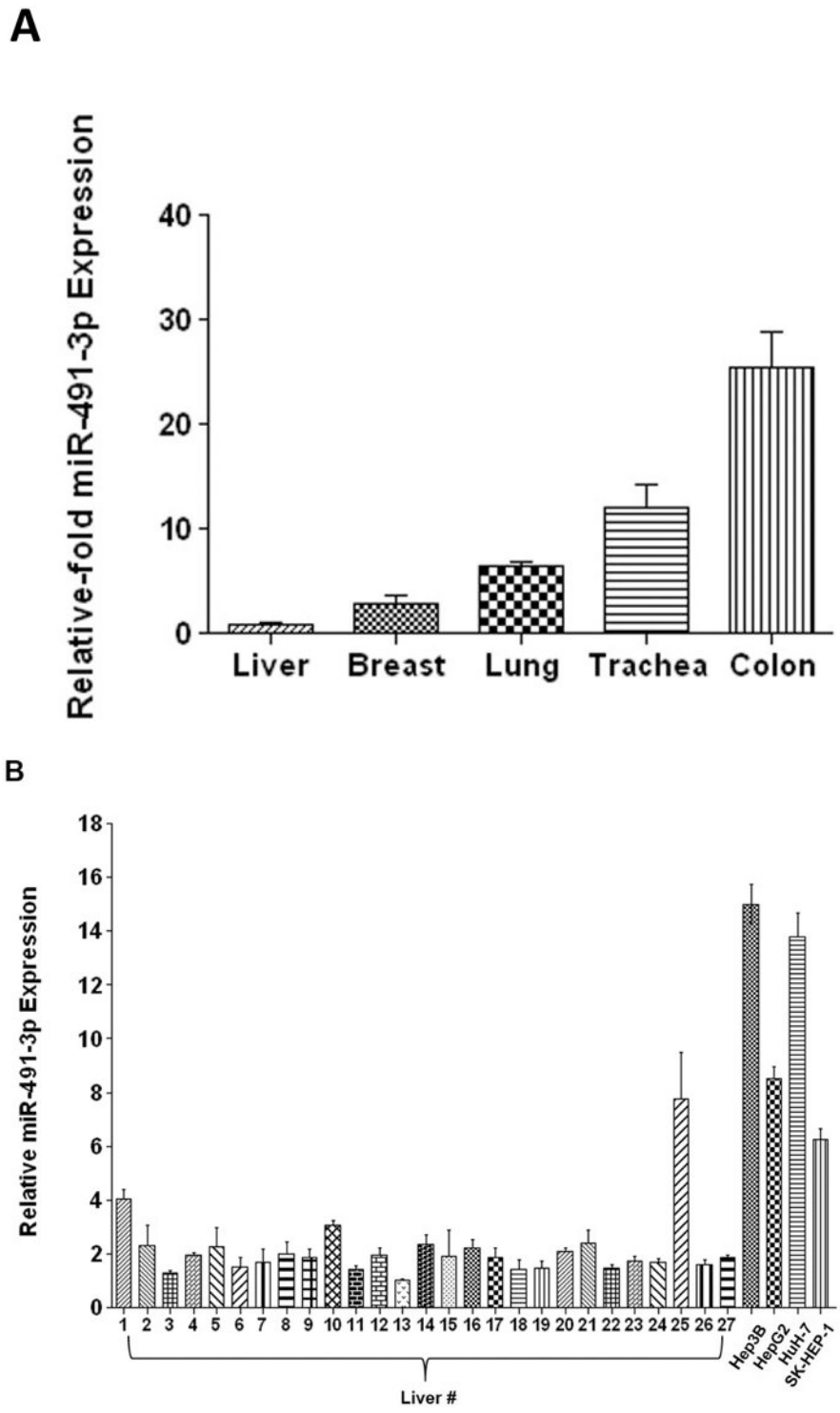

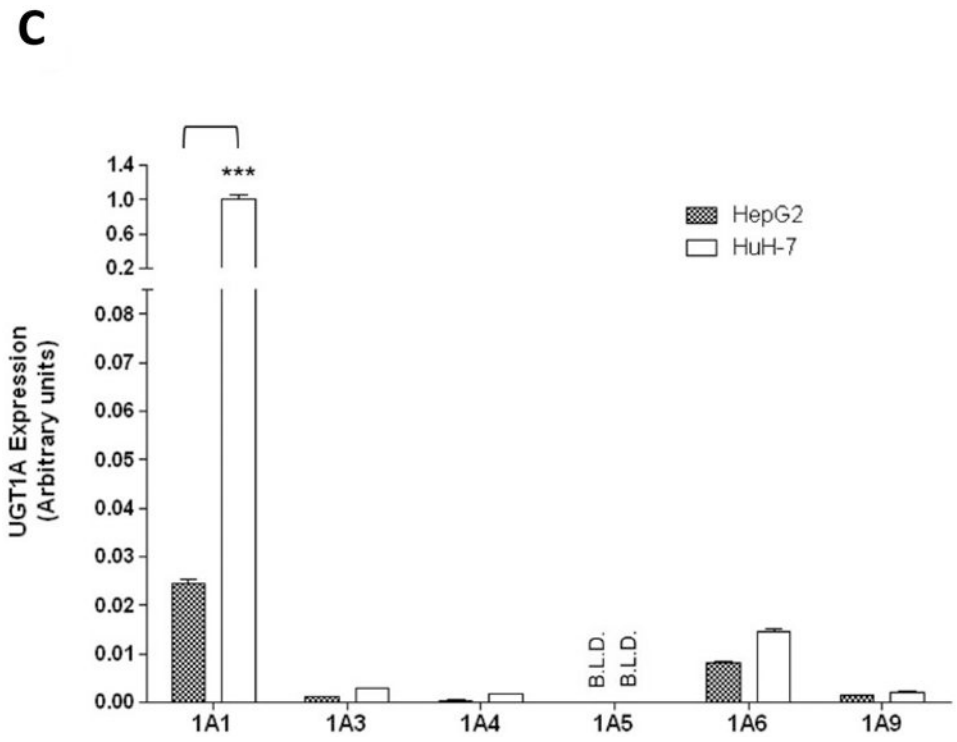

Figure 2. Tissue and cell line expression of miR-491–3p and UGT1A family members.

A, Relative expression levels of miR-491–3p in several UGT-expressing tissues. Expression levels were quantified using qRT-PCR and set relative to the lowest-expressing tissue (i.e. liver). *B,* Expression levels of mature miR-491–3p in individual normal livers and in liver cancer cell lines. Expression levels were quantified by qRT-PCR. miR-491–3p expression was adjusted to the RNU6B endogenous control gene in all tissues and cell lines. Expression is shown relative to the lowest overall miR-491–3p-expressing sample (i.e. liver #13; set to 1.0). *C,* Comparison of UGT1A mRNA levels between HepG2 and HuH-7 cell lines. mRNA expression was adjusted to the RPLPO endogenous control gene and shown relative to the highest expressing UGT enzyme in both cell lines (UGT1A1 in HuH-7 cells; set to 1.0). The Y-axis is broken into two segments, with a gap between 0.08 and 0.2 to better adjust for the high expression of UGT1A1 in HuH-7 cells. UGT1A1 mRNA levels were >40-fold higher in HuH-7 cells compared to HepG2. *B.L.D.,* below the limit of detection. Columns represent the mean ± S.E. of three independent replicates. *** $P<0.001$.

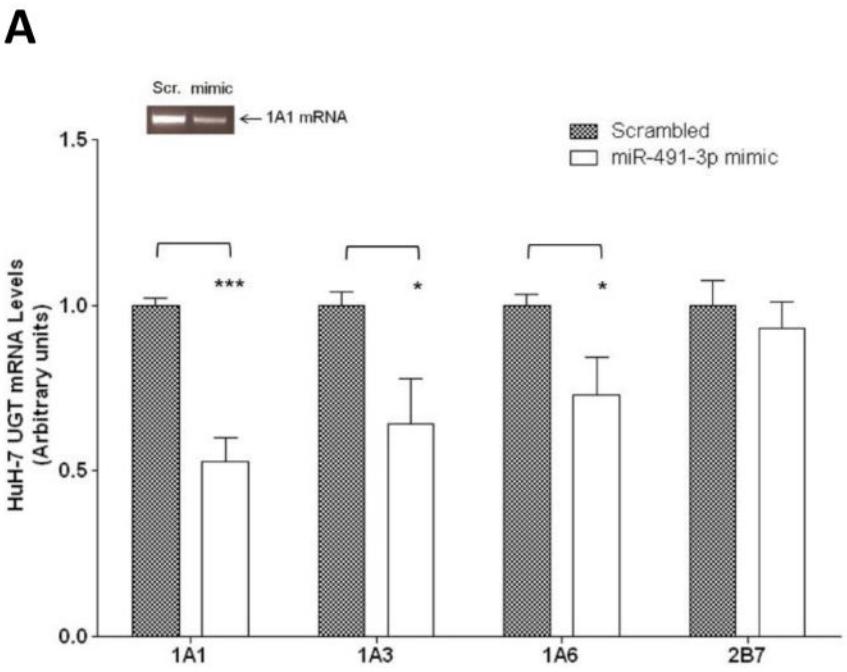

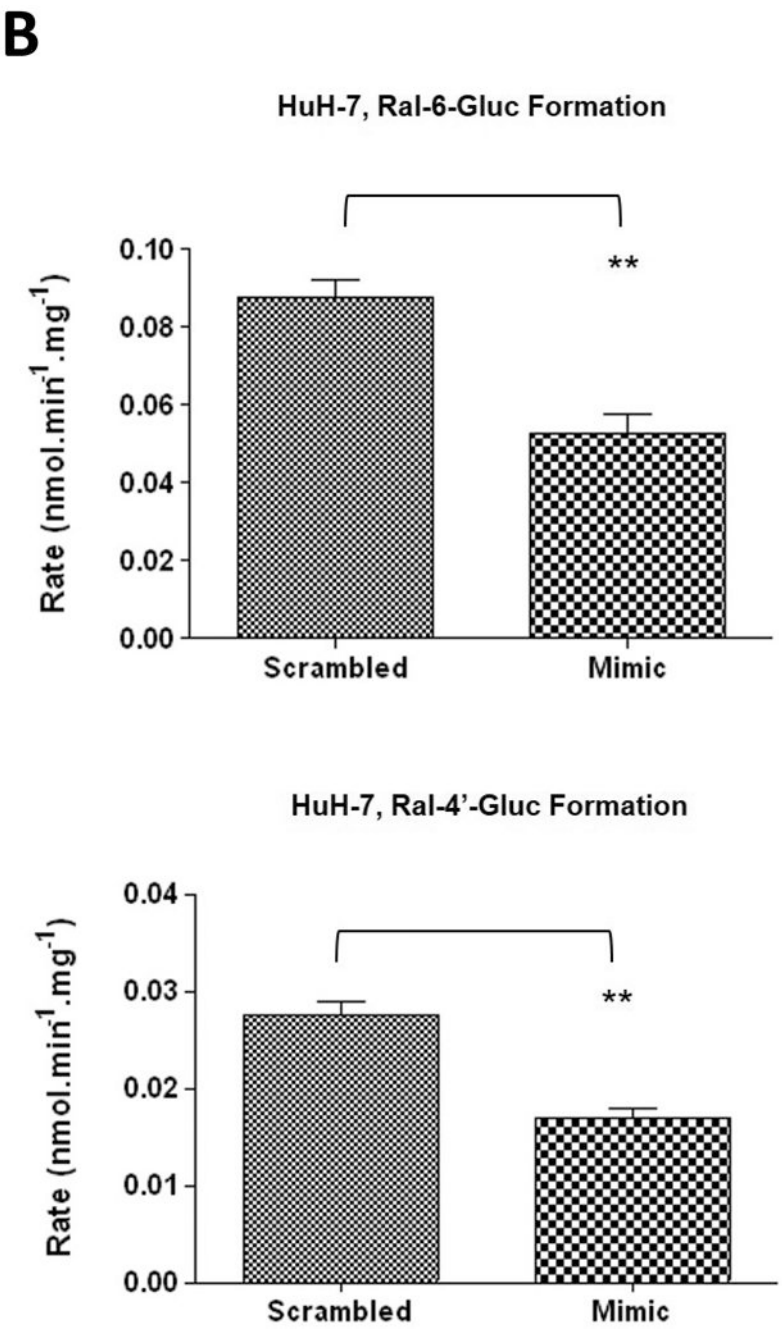

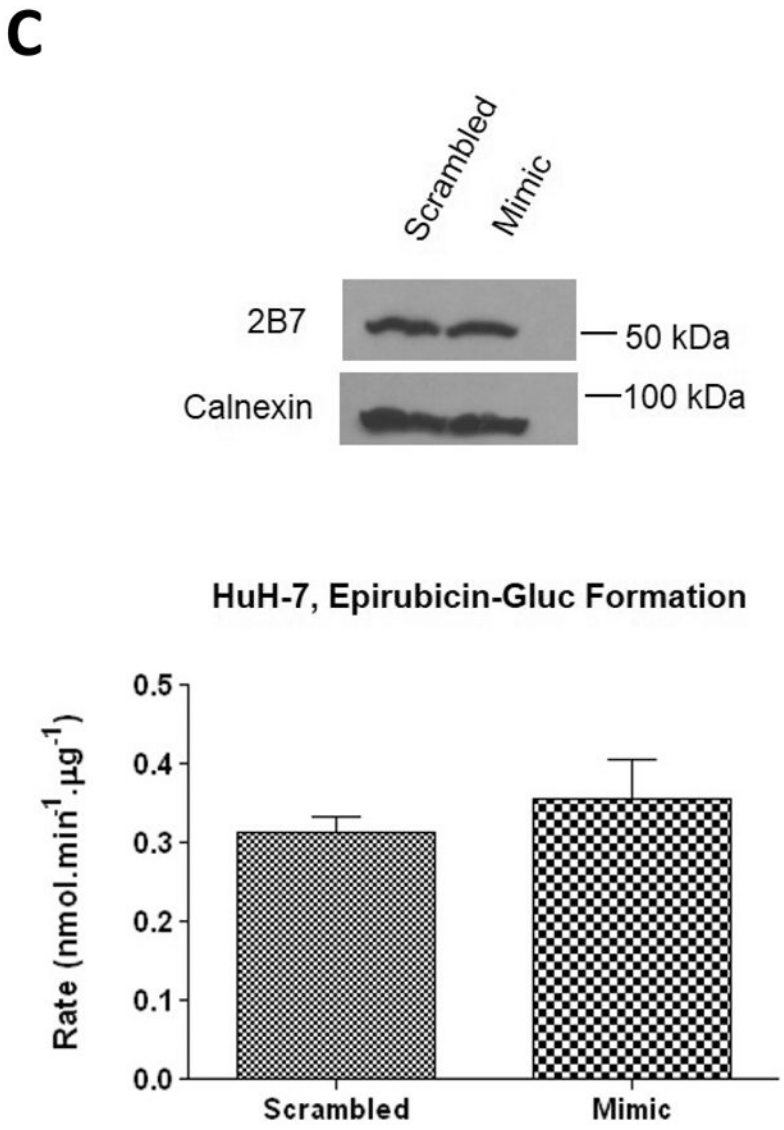

Figure 3. Quantitative analysis of UGT1A mRNA and enzymatic activity in HuH-7 cells.

A, mRNA levels of UGT1A1, 1A3, 1A6, and 2B7 in miR-491–3p transfected HuH-7 cells. 50 nM of scrambled miRNA or miR-491–3p mimic were transiently transfected into HuH-7 cells for 48 h. mRNA was isolated and levels were compared to scrambled control (set at 1.0) for each gene. Genes were normalized to the RPLPO endogenous control gene using the $2^{-\Delta\Delta ct}$ method. UGT2B7 mRNA levels served as a negative control. Inset, a representative semi-quantitative electrophoresis gel of UGT1A1 mRNA. *B,* UGT1A1 glucuronidation activity against raloxifene in HuH-7 cells. UPLC/MS/MS was used to quantify the formation of ral-6-gluc (top) and ral-4'-gluc (bottom) from raloxifene substrate in miRNA-transfected HuH-7 homogenates. Ral-6-gluc formation and ral-4'gluc formation were significantly repressed ~40% and ~38%, respectively. *C,* UGT2B7 protein levels and glucuronidation activity in the presence of 50 nM miR-491–3p miRNA mimic or scrambled control. Columns represent the mean ± S.E. of three independent experiments. * $P<0.05$; ** $P<0.01$; *** $P<0.001$.

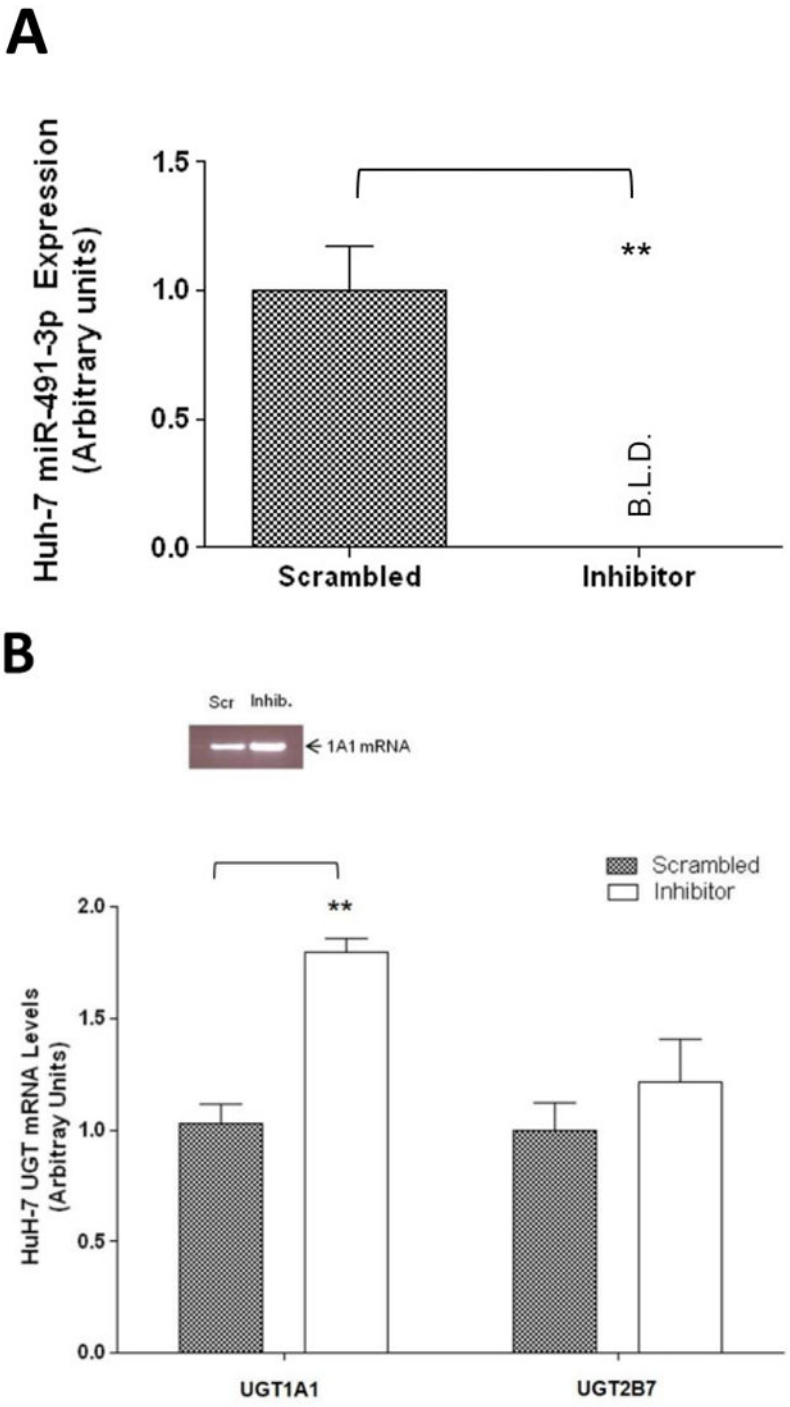

C

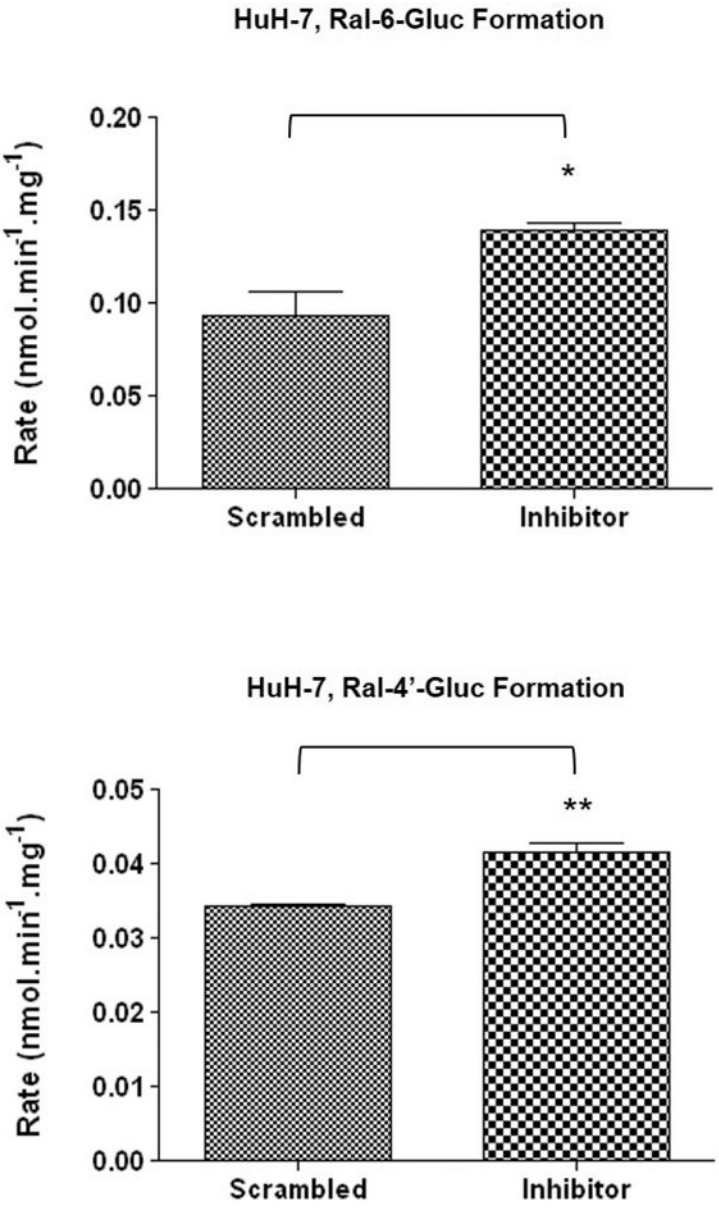

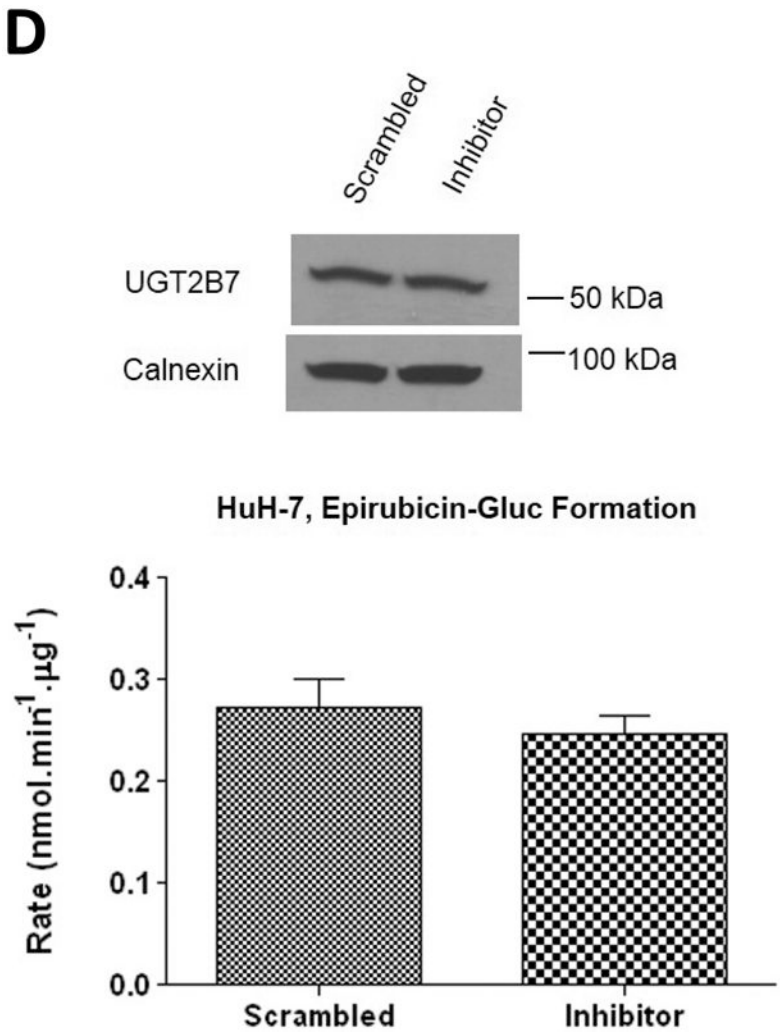

Figure 4. The effect of miR-491–3p inhibitor on UGT1A1 expression and activity in HuH-7 cells.

A, 100 nM of scrambled inhibitor control or miR-491–3p inhibitor were transiently transfected into HuH-7 cells for 48 h. Quantitative analysis of endogenous mature miR-491–3p expression levels were measured following miRNA isolation from transfected HuH-7 cells using qRT-PCR with RNU6B as an endogenous control. *B,* Quantification of UGT1A1 and UGT2B7 mRNA levels by qRT-PCR in HuH-7 cells in the presence of 100 nM miR-491–3p inhibitor or scrambled control. Quantification was performed with RPLPO serving as the endogenous expression control gene using the $2^{-\Delta\Delta ct}$ method. Inset, a representative electrophoresis gel of the RT-PCR of UGT1A1 mRNA levels. *C,* UGT glucuronidation activity against raloxifene in HuH-7 cells with inhibited miR-491–3p. UPLC/MS/MS was used to quantify the formation of ral-6-gluc (top) and ral-4'-gluc (bottom) from raloxifene substrate in miR-491–3p-inhibited HuH-7 cell homogenates. *D,* UGT2B7 protein levels and glucuronidation activity in the presence of 100 nM miR-491–3p miRNA mimic or scrambled control. Columns represent the mean ± S.E. of three independent experiments. B.*L.D.,* below the limit of detection. * $P<0.05$; ** $P<0.01$.

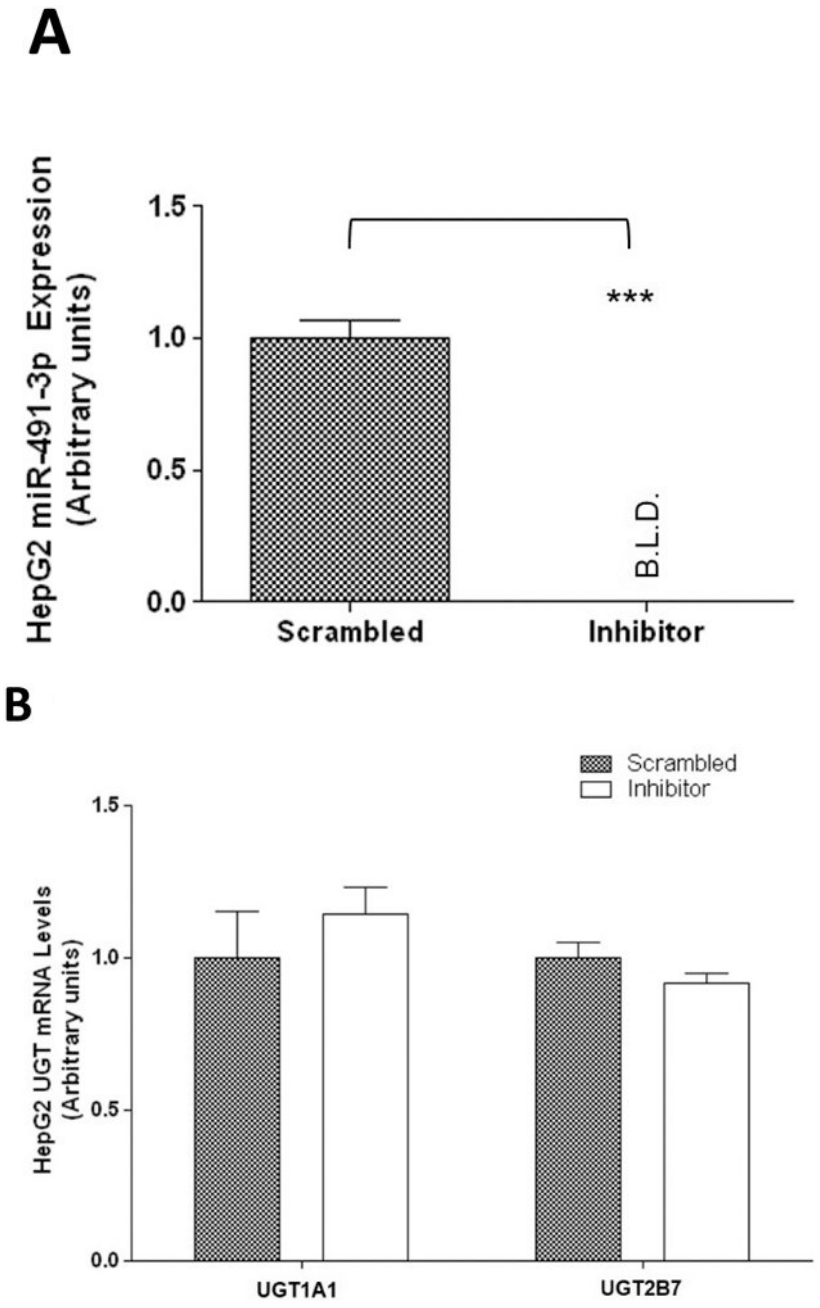

C

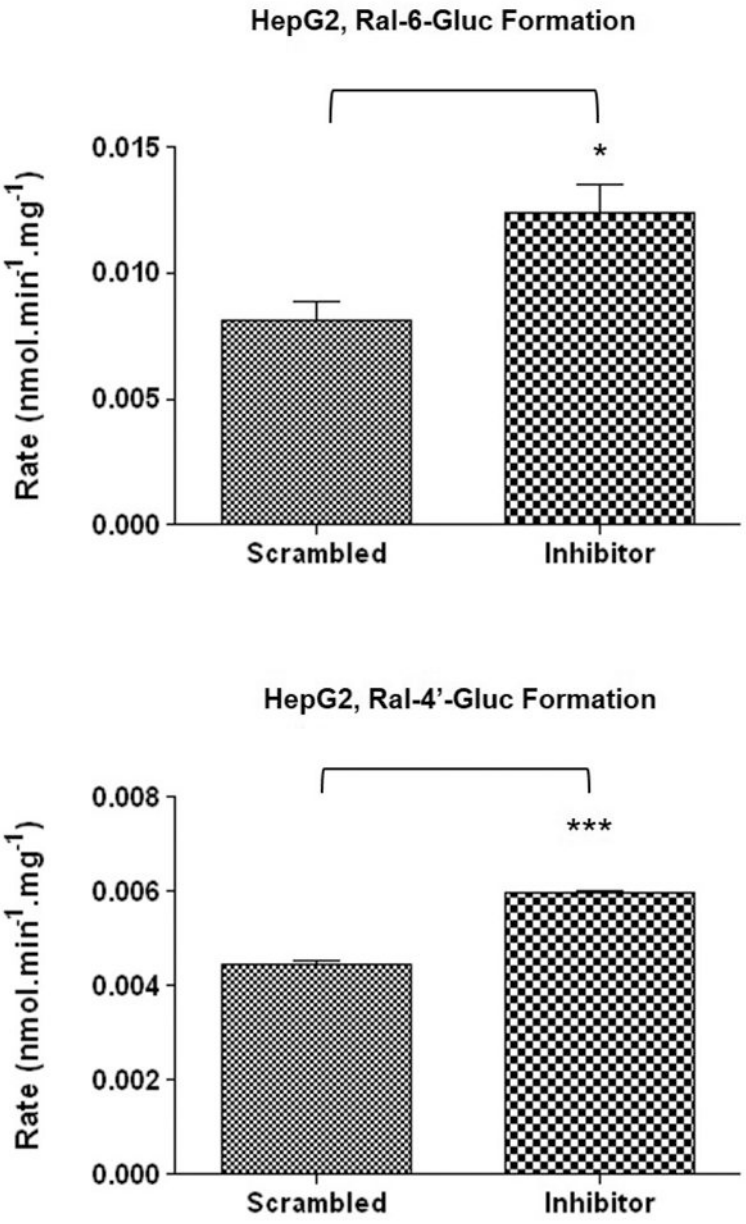

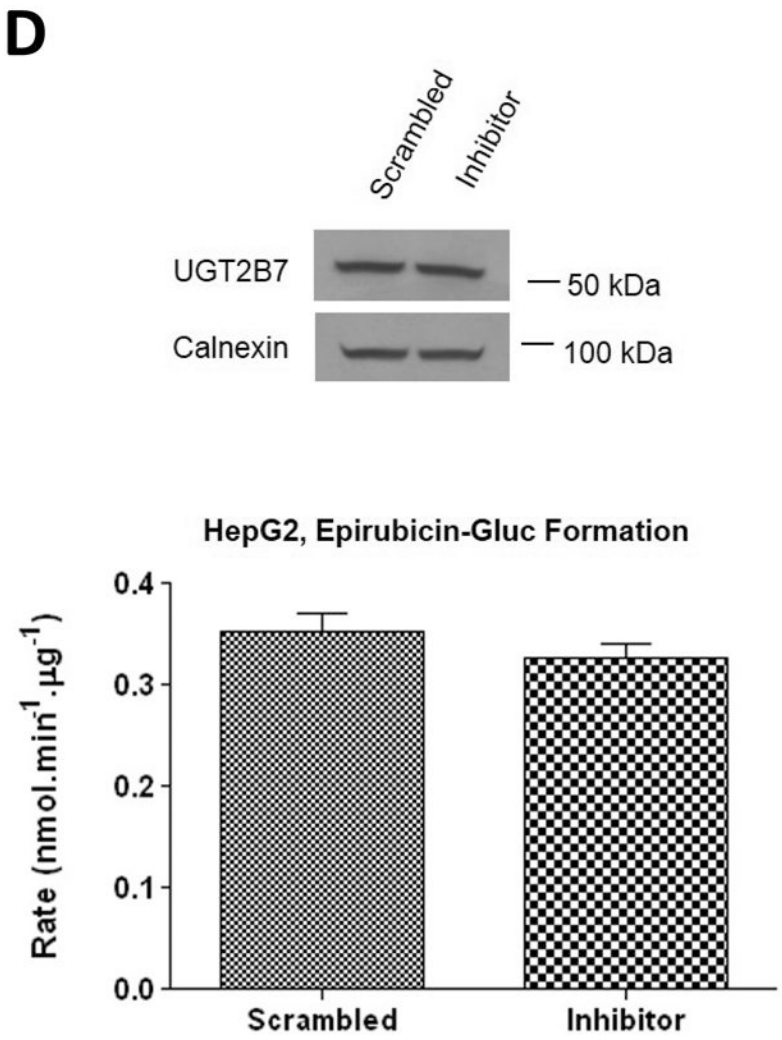

Figure 5. The effect of miR-491–3p inhibitor on UGT1A1 expression and activity in HepG2 cells.

A, One hundred nM scrambled inhibitor control or miR-491–3p inhibitor were transiently transfected into HepG2 cells for 48 h. Quantitative analysis of endogenous mature miR-491–3p expression levels were measured following miRNA isolation from transfected HepG2 cells using qRT-PCR and the RNU6B endogenous control. *B,* Quantification of UGT1A1 and UGT2B7 mRNA levels by qRT-PCR in HuH-7 cells in the presence of 100 nM miR-491–3p inhibitor or scrambled inhibitor control. Quantification was performed with RPLPO serving as the endogenous expression control gene using the $2^{-\Delta\Delta ct}$ method. *C,* UGT glucuronidation activity against raloxifene in HepG2 cells with inhibited miR-491–3p. UPLC/MS/MS was used to quantify the formation of ral-6-gluc (top) and ral-4'-gluc (bottom) from raloxifene substrate in miR-491–3p- inhibited HepG2 cell homogenates. *D,* UGT2B7 protein levels and glucuronidation activity in the presence of 100 nM miR-491–3p miRNA inhibitor or scrambled inhibitor control. Columns represent the mean ± S.E. of three independent experiments. B.*L.D.,* below the limit of detection. * $P<0.05$; *** $P<0.001$.

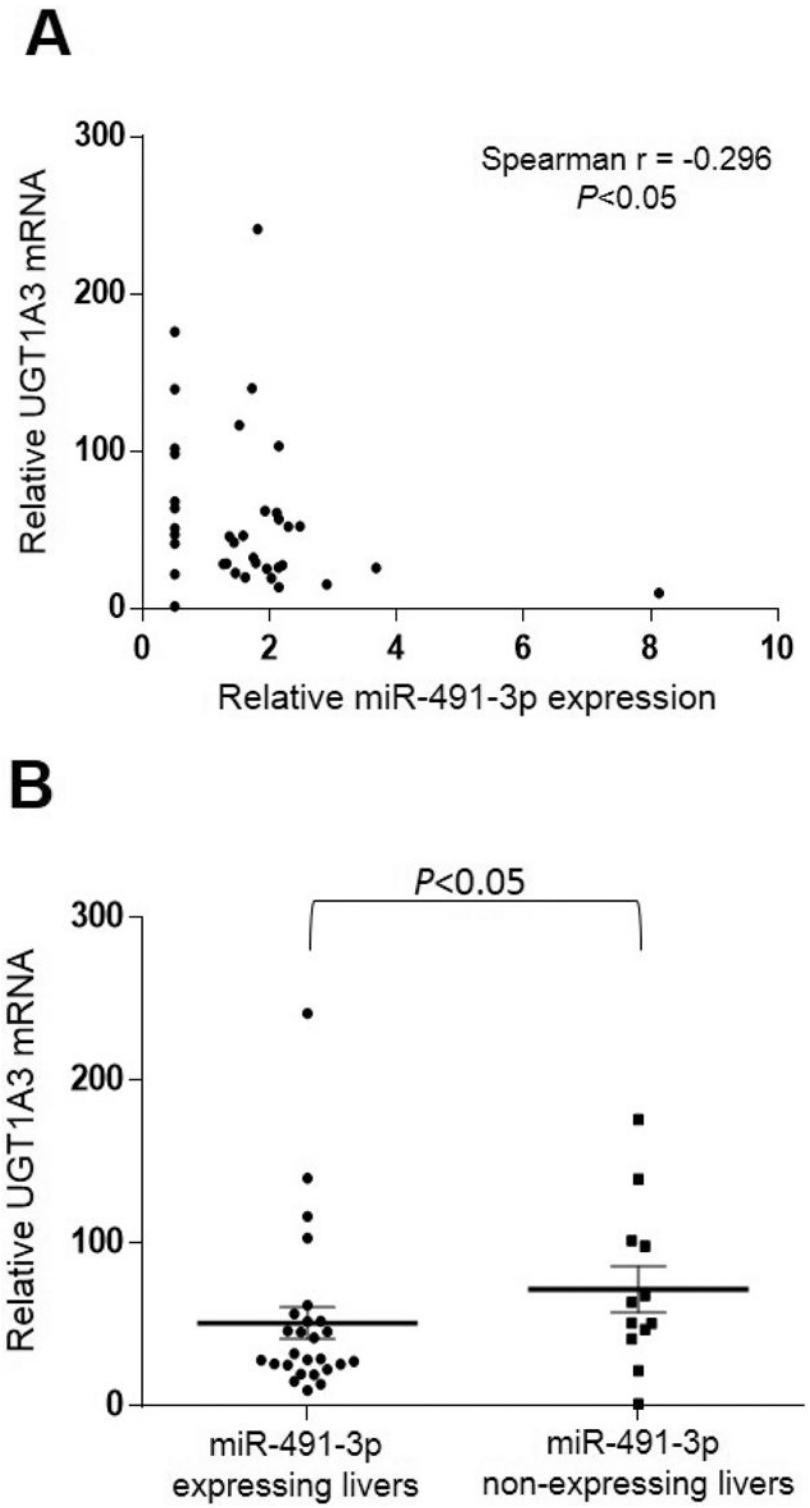

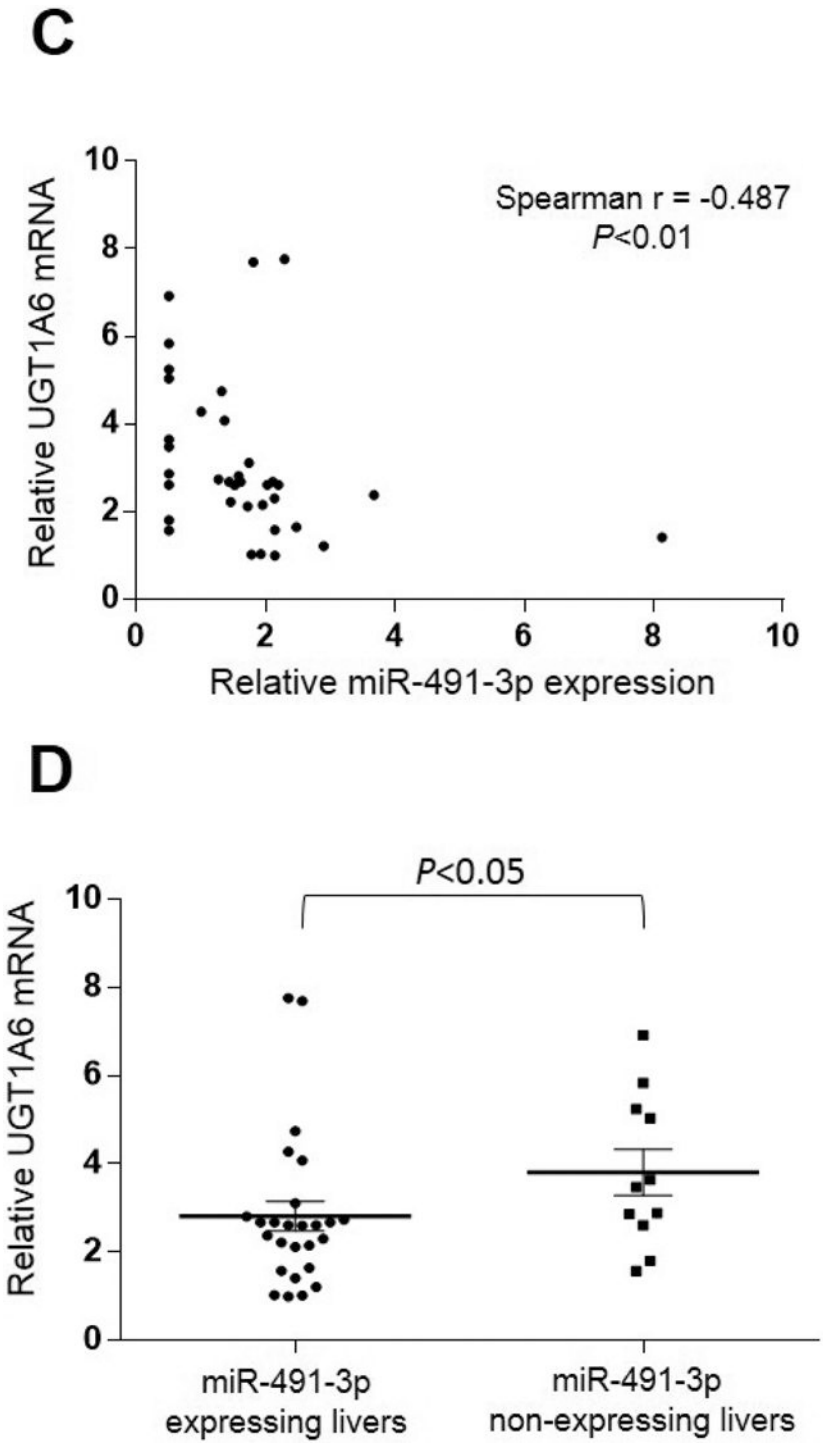

Figure 6. Expression of UGT1A3 and UGT1A6 mRNA versus miR-491–3p in human liver specimens.

Levels of UGT1A3 (n=38; panels *A* and *B*) and UGT1A6 (n=37; panels *C* and *D*) mRNA vs. miR-491–3p were quantified in normal liver samples via qRT-PCR and normalized to RPLPO and RNU6B, respectively. For panels *A* and *B*, expression levels are shown relative to the lowest expressing sample (set to 1.0) for each gene, with those specimens with no

miR-491–3p expression assigned a Ct value half that of the lowest miR-491–3p expressing liver specimen. *A,* UGT1A3 mRNA vs. miR-491–3p expression was examined using the Spearman ranking method. *B,* UGT1A3 mRNA expression levels were examined in liver specimens stratified by expression vs. no expression of miR-491–3p. *C,* UGT1A6 mRNA vs. miR-491–3p expression was examined using the Spearman ranking method. *D,* UGT1A6 mRNA expression levels were examined in liver specimens stratified by expression vs. no expression of miR-491–3p. Dots represent the mean ± S.E. of three independent replicates.